ROLE OF FAM134B IN LIVER CANCER

A THESIS SUBMITTED TO
THE DEPARTMENT OF MOLECULAR BIOLOGY AND GENETICS
AND THE GRADUATE SCHOOL OF ENGINEERING AND SCIENCE OF
BILKENT UNIVERSITY
IN PARTIAL FULFILLMENT OF THE REQUIREMENTS
FOR THE DEGREE OF
MASTER OF SCIENCE

BY

AYŞE DERYA SONER

AUGUST 2013

I certify that I have read this thesis and that in my opinion it is fully adequate, in scope and in quality, as a thesis for the degree of Master of Science.

Prof. Dr. Mehmet Öztürk

I certify that I have read this thesis and that in my opinion it is fully adequate, in scope and in quality, as a thesis for the degree of Master of Science.

Assoc. Prof. Dr. Rengül Çetin-Atalay

I certify that I have read this thesis and that in my opinion it is fully adequate, in scope and in quality, as a thesis for the degree of Master of Science.

Assist. Prof. Dr. Arzu Atalay

Approved for the Graduate School of Engineering and Science

Prof. Dr. Levent Onural
Director of the Graduate School of
Engineering and Science

ABSTRACT

ROLE OF FAM134B IN LIVER CANCER

Ayşe Derya Soner
M.Sc. in Molecular Biology and Genetics
Supervisor: Prof. Dr. Mehmet Öztürk
August 2013, 74 Pages

The family with sequence similarity 134, member B (FAM134B) protein initially caught attention in our laboratory through demonstrating elevated levels possibly associated with senescent, cirrhotic, and mesenchymal-like states in hepatocellular carcinoma (HCC), and the aim of this thesis work was to identify the role of FAM134B in HCC. The work in this thesis initially demonstrated that the induction of endoplasmic reticulum (ER) stress in normal mice livers with 8 hours of tunicamycin treatment did not significantly alter the levels of FAM134B mRNA or protein. We then demonstrated that induction of ER stress in four HCC cell lines using several ER stress inducers such as thapsigargin, tunicamycin or DTT did not cause a significant increase in the levels of FAM134B mRNA or protein, with the exception of high dose DTT treatment of Snu449 cells which also demonstrated apoptosis. We also observed that FAM134B protein levels may be elevated during epithelial-to-mesenchymal transition (EMT) in PLC cells induced by TGF-β treatment. Snu449 cells in which FAM134B was silenced demonstrated an altered morphology in cell culture, and appeared to lose their migratory capabilities. Most significantly though, FAM134B-silenced Snu449 cells demonstrated a dramatic loss of resistance to treatment with thapsigargin and adriamycin, which are both known to inhibit the calcium pumps on the ER. The knockdown cells also demonstrated loss of resistance to serum starvation, TGF-β treatment, tunicamycin and alcohol treatment, but no significant difference was observed in resistance to 5-FU, camptothecin and hydrogen peroxide. These results implicated that FAM134B may play a role that is essential for survival under several forms of cytotoxic threat, especially those that disturb calcium homeostasis.

ÖZET

FAM134B'NİN KARACİĞER KANSERİNDEKİ ROLÜ

Ayşe Derya Soner
Moleküler Biyoloji ve Genetik Yüksek Lisansı
Tez Yöneticisi: Prof. Dr. Mehmet Öztürk
Ağustos 2013, 74 Sayfa

FAM134B (family with sequence similarity 134, member B) isimli protein laboratuarımızda ilk olarak seviyelerinin artışı hepatosellüler karsinomda hücre yaşlanması, siroz ve mezenkimal benzeri davranış durumları ile bağlantılı olabilecek bir protein olarak dikkat çekti, ve bu tez çalışmasının amacı FAM134B'nin hepatosellüler karsinomdaki rolünü tanımlamaktı. Bu tezdeki çalışmalar ilk olarak normal fare karaciğerinde 8 saatlik tünikamisin uygulamasi ile indüklenen endoplazmik reticulum (ER) stresinin, FAM134B mRNA ve protein seviyelerine önemli bir etkisi olmadığını gösterdi. Daha sonra da tapsigargin, tunikamisin ve DTT gibi indukleyiciler kullanılarak oluşturulan ER stresinin dört hepatosellüler karsinom hücre hattında da FAM134B mRNA ve protein seviyelerine önemli bir etkisi olmadığını gösterdik; tek istisnai durum yüksek doz DTT uygulanan ve hücre ölümü gösteren Snu449 hücreleri idi. Bunların yanısıra, FAM134B protein seviyelerinin PLC hücrelerinde TGF-β ile indüklenen epitel-mezenkimal geçiş sırasında da artıyor olabileceğini gözlemledik. FAM134B'nin susturulduğu Snu449 hücrelerinin kültürde farklı bir morfolojiye sahip olduklarını, ve hareket kabiliyetlerini yitirdiklerini gözlemledik. Fakat en önemlisi, FAM134B'nin susturulduğu Snu449 hücreleri, tapsigargin ve adriamisin uygulamasına olan dirençlerini çok ciddi bir şekilde kaybettiler, ve bu iki ilacın da ER membranındaki kalsiyum pompalarının çalışmasına engel oldukları biliniyor. FAM134B'nin susturulduğu hücreler aynı zamanda serum yetersizliği, TGF-β, tunikamisin ve alkol uygulamalarına olan dirençlerinde de kayıp gösterdiler, fakat 5-FU, camptotesin ve hidrojen peroksite olan dirençlerinde ciddi bir değişim gözlenmedi. Bu sonuçlar, FAM134B'nin hücre ölümüne neden olabilecek (özellikle de kalsiyum dengesinin bozulması gibi) birçok durumda hücrenin hayatta kalma mekanizmasında önemli bir rol oynayabileceğini gösteriyor.

To my precious family...

ACKNOWLEDGEMENTS

This thesis work has been made possible by the scientific guidance and emotional support of many people.

First and foremost, I would like to thank my thesis supervisor Prof. Dr. Mehmet Öztürk for his great scientific vision; the perspectives he preferred to pursue during this research work steered us towards very interesting findings. I have had the great fortune of working in Prof. Öztürk's laboratory starting with my senior projects, and I have learned a lot from him throughout these past three years; I am very thankful for all his scientific guidance, fatherly advice, and his encouraging, positive attitude towards his students.

As an extension of our supervisor's motivating attitude, the Öztürk lab has always been a place of hard work, as well as lots of laughs, support, and sharing. I am very grateful to have had the blessing of working with the past and present members of our group; Dr. Ceyhan Ceran, Dr. Pelin Telkoparan, Dr. Çiğdem Özen, Dr. Hani Alotaibi, Mustafa Yılmaz, Dilek Çevik, Ayşegül Örs, Gökhan Yıldız, Umur Keleş, Hande Topel, Alper Dağcan, Yusuf İsmail Ertuna, Emre Yurdusev, Engin Demirdizen, Merve Deniz Abdüsselamoğlu, Umar Raza and Dr. Ayaz Mustufa have all been great people to work with, and have provided lots of support.

I am also very grateful to all past and present Bilkent MBG faculty members; I was lucky to have the chance to meet them all and I learned a lot from them over the past six years. I have learned a lot from Assist. Prof. Dr. Ebru Erbay, especially during the endoplasmic reticulum stress-related section of this thesis work. Assoc. Prof. Işık Yuluğ, Assoc. Prof. Rengül Çetin-Atalay and Assist. Prof. Özlen Konu have not only taught me a lot about molecular biology, but have also always provided motherly support and advice. I was also lucky enough to receive the support and advice of Assoc. Prof. Uygar Tazebay, for which I am also very grateful. I have also learned a lot from Prof. Can Akçalı, Assoc. Prof. İhsan Gürsel, Assist. Prof. Ali Güre, Prof. Tamer Yağcı, and Prof. Tayfun Özçelik, both inside and outside the classroom. Further members of the MBG family have also been of great help throughout this

thesis work; I am very thankful to Bilge Kılıç, Füsun Elvan, Sevim Baran, Yıldız Karabacak, Abdullah Ünnü, Turan bey and Ümmühan hanım for their patience.

The MBG family has always felt like an actual family, and I am very lucky to have worked among such friends. I am especially grateful for having the friendship and support of Damla Gözen, Merve Çakır, Şahika Cıngır, Mehmet Şahin, Sıla Özdemir, Büşra Yağabasan and Özlem Tufanlı throughout this thesis work; they have been more like sisters and brothers to me than friends. I am also very grateful for the great support I received from my family, my parents, my sister, and Ömer Faruk Cavga, who have always helped me through the times of hard work.

Finally, I would like to thank the Scientific and Technological Research Council of Turkey (TÜBİTAK) for providing the grants that have made this research work possible, through funding project numbers 101S191 and 111T558.

TABLE OF CONTENTS

LIST OF TABLES

LIST OF FIGURES

1. INTRODUCTION

1.1 Cancers of the Liver; Status Worldwide & in Turkey

Cancer is a leading cause of death worldwide, and although the most common incidences are cancers of the breast, prostate and lung, liver cancers draw attention with the second poorest survival rates, preceded only by cancers of the pancreas, as shown in Figure 1.1 [1] .

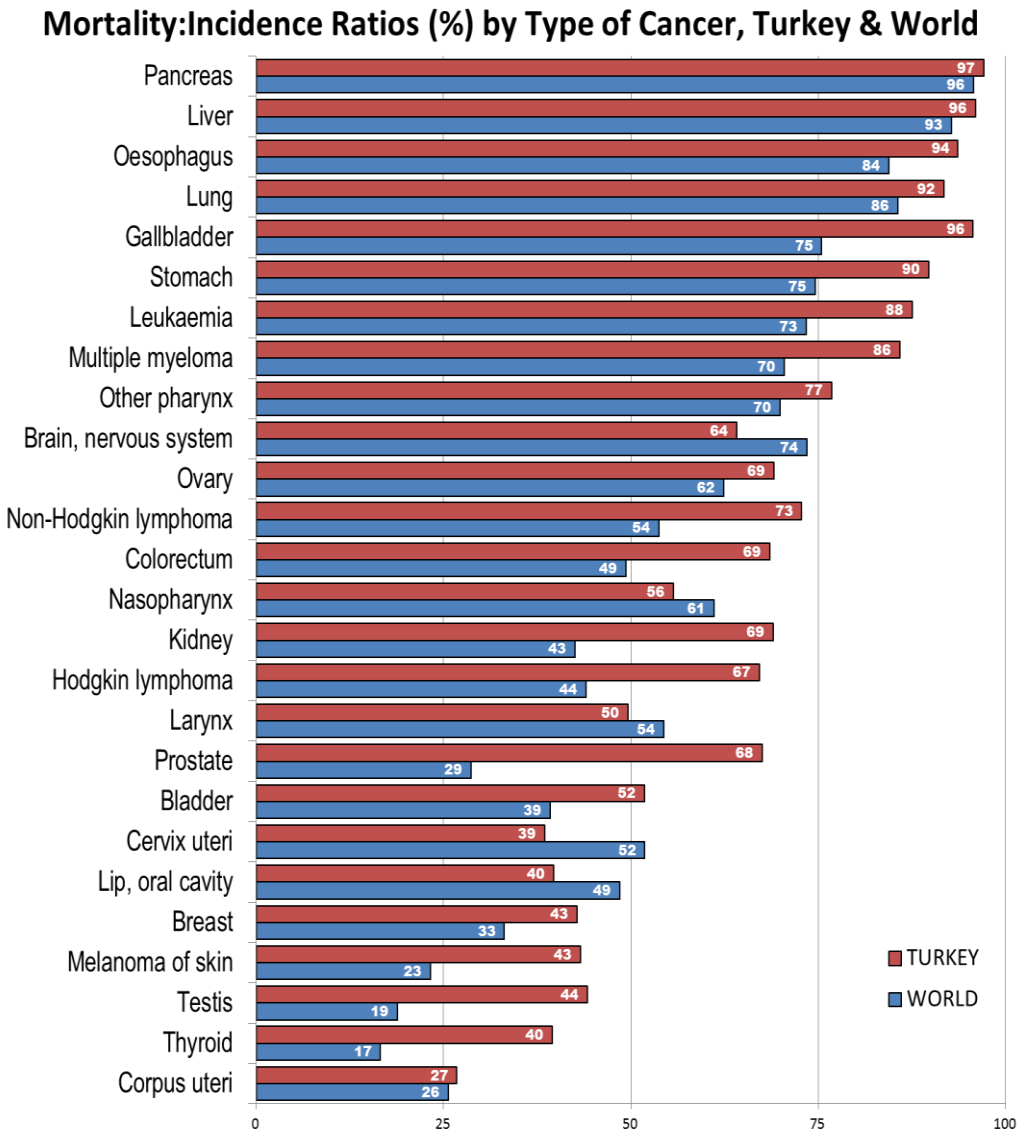

Figure 1.1: Mortality-to-incidence ratios of cancers in Turkey and Worldwide.

Data obtained from GLOBOCAN 2008 Cancer Fact Sheet [1]

As demonstrated in Figure 1.1, 93% of liver cancer patients do not survive this disease, while this ratio is 86% for lung cancers, and 33 and 29% for cancers of the breast and prostate respectively. These high fatality rates make liver cancer the third most common cause of death from cancers worldwide, causing 600,000 deaths per year, although it is the seventh most common type of cancer [2] [3].

These poor survival rates associated with cancers of the liver are caused by difficulties in timely diagnoses and inoperability of the tumors; most cases are diagnosed when the tumor has passed the localized state and reached the distant stage, [4] and only 10-20% of the tumors can be removed completely by surgery [5]. For the time being, the best treatment for liver cancer is liver transplantation, but it can be offered only to patients with small tumors and is limited by the availability of organ donors [6]. The prognostic outcome is better in more developed countries where more advanced facilities are available for both diagnosis and treatment [3].

A significant ratio of liver cancers is attributable to infection by hepatitis B virus (HBV), for which vaccination is available; the ratio of liver cancers caused by HBV infection is 60% in developing countries and 23% in developed countries [3]. The World Health Organization is promoting a vaccination program, and 177 countries have integrated the HBV vaccine to their national infant immunization schedules as of 2008 [3]. Hepatitis C virus (HCV) infection, on the other hand, accounts for 33% of liver cancers in developing countries and for 20% in developed countries, however, vaccination is not possible thus far [3].

Importantly, despite the implementation of preventative measures such as vaccination programs, the incidence rates of liver cancers are still increasing in many regions, including Central Europe and the United States, and this increase is partly attributable to the increasing rates of obesity [3].

This worrying state draws attention to the mechanisms involved on the contribution of obesity and other non-viral factors on the onset and progression of cancers of the liver; obesity, metabolic syndrome, diabetes, exposure to aflatoxins, and alcohol consumption constitute an aspect of liver cancers for which the endoplasmic reticulum (ER) appears to play key roles, and these will be discussed in detail.

1.2 Hepatocellular Carcinoma

Hepatocellular carcinoma (HCC) is the most common type of liver cancer, making up 70% to 85% of all primary liver cancers worldwide [3]. Rarer forms of liver cancer include hepatoblastoma, angiosarcoma or cholangiocarcinoma [7].

The liver is one of the major secretory organs of the human body, and hepatocytes constitute approximately 80% of the total mass of this organ; these cells are the main functional cells of the liver, and have essential roles in the synthesis and storage of many proteins, the metabolisms of carbohydrates and lipids, synthesis phospholipids, cholesterol and bile salts, and detoxification of drugs and toxins [8].

Both the dedifferentiation of mature hepatocytes and imperfect differentiation of hepatic progenitor cells (HPCs) appear to contribute to hepatocarcinogenesis [9] during the attempt of the liver to make up for hepatocytes lost by persistent damage; the mechanisms involved will be discussed in further detail.

1.3 Pathogenesis of Hepatocellular Carcinoma

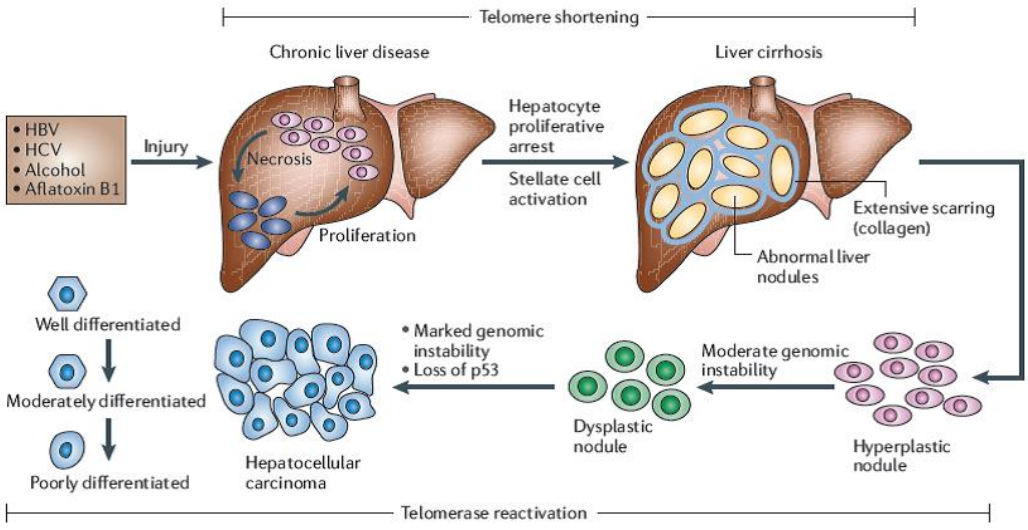

Figure 1.2 Histopathological progression and molecular features of HCC. [12]

Risk factors leading to hepatocarcinogenesis include viral infections such as Hepatitis B (HBV) and Hepatitis C (HCV) infections, metabolic conditions such as obesity, non-alcoholic fatty liver disease and diabetes, toxic factors such as alcohol

and aflatoxins, as well as other factors such as autoimmune hepatitis and hereditary haemochromatosis [10][11][12]. These factors can directly cause DNA damage, mutations and epigenetic irregularities involving oncogenes and tumor suppressor genes, telomerase activation and chromosomal abnormalities. Moreover, persistent damage to hepatocytes also contribute to carcinogenesis through causing hepatocyte death either via apoptosis or via necrosis, which, in turn, leads to the development of chronic liver disease, fibrosis, and cirrhosis [13]. It is important to note that 80% of HCC cases are observed in patients that initially experience chronic liver disease and cirrhosis [14].

As a way to make up for cell death, the liver cells start regenerating, and this involves high rates of cell division and proliferation. As demonstrated in Figure 1.2, this high rate of proliferation leads to telomere shortening and genomic instability [12]. The high rates of DNA replication may also make the cells more prone to errors and the accumulation of mutations.

Most frequently reported molecular causes of aberrant proliferation and dedifferentiation of hepatocytes include; inactivation of tumor suppressors such as p53, retinoblastoma protein (pRb) or the $p14^{ARF}$ and $p16^{INK4a}$ proteins encoded by the CDKN2A gene, overexpression of oncogenes such as CyclinD1/Cdk4, insulin-like growth factor-II or c-MET, and activation of Ras/mitogen activated protein (MAPK), transforming growth factor-β (TGF- β) or Wnt/ β-catenin signaling cascades [15].

1.3.1 Fibrosis as an Initial state of Hepatocarcinogenesis

Damage to hepatocytes may be caused by several factors such as elevated metabolic overload resulting in high levels of reactive oxygen species (ROS) and ER stress, chemical toxicity by drugs, alcohol or aflatoxins, or viral activity causing metabolic deregulation [16].

Steatosis, which involves the expanding of hepatocytes due to excessive lipid droplet storage, is one of the first signs of cellular stress, and is highly reversible. Irreversible or persistent damage, however, may cause hepatocyte death through apoptosis or necrosis. The death-mediated signals trigger the activation of Kupffer

and quiescent hepatic stellate cells which coordinate an inflammatory and wound healing response; Kupffer cells are specialized macrophages of the liver, and stellate cells are pericytes involved in formation of scar tissue. As illustrated in Figure 1.3, in an acute setting, this response might lead to tissue regeneration and repair, however, when the injury is chronic, the consequences are fibrogenesis, cirrhosis, and cancer [13].

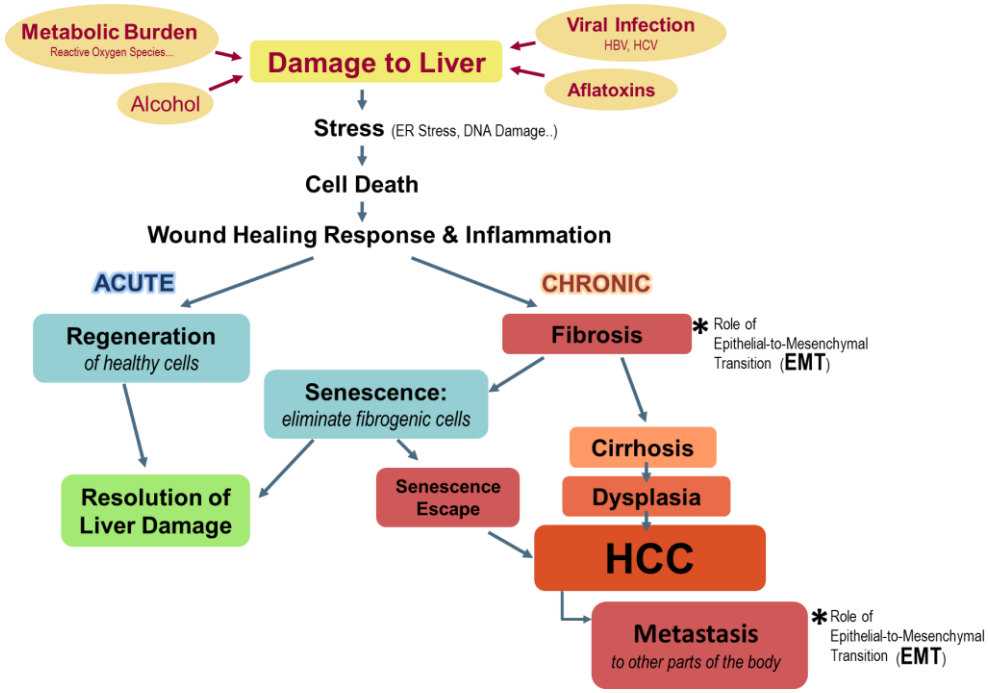

Figure 1.3: **The progression of hepatocellular carcinoma & the role of senescence as a means of eliminating fibrotic cells.** *Adapted from Dooley & Ten Dijke, 2012* [13]

Fibrosis is the scarring of a tissue due to excessive deposition of extracellular matrix (ECM) proteins as an attempt of repair. During chronic liver injury, the quiescent hepatic stellate cells become activated by signals described in Figure 1.4, such as inflammatory cytokines and give rise to myofibroblasts. Myofibroblasts are the cell type responsible for fibrosis in the liver [13].

As also shown in Figure 1.4, transforming growth factor-β (TGF-β) is considered one of the major pro-fibrogenic cytokines, as demonstrated by data obtained from animal models of liver damage [13]. In fact, TGF-β plays important roles in many stages of liver disease, which will be discussed in detail.

Although majority of evidence suggests that hepatic stellate cells are the main contributors of the myofibroblast build that forms during fibrogenesis, there is evidence that other cell types such as portal fibroblasts of the liver, bone-marrow-derived fibrocytes, or circulating mesenchymal cells may also contribute to the fibrosis through deposition of extracellular matrix proteins [13] [17].

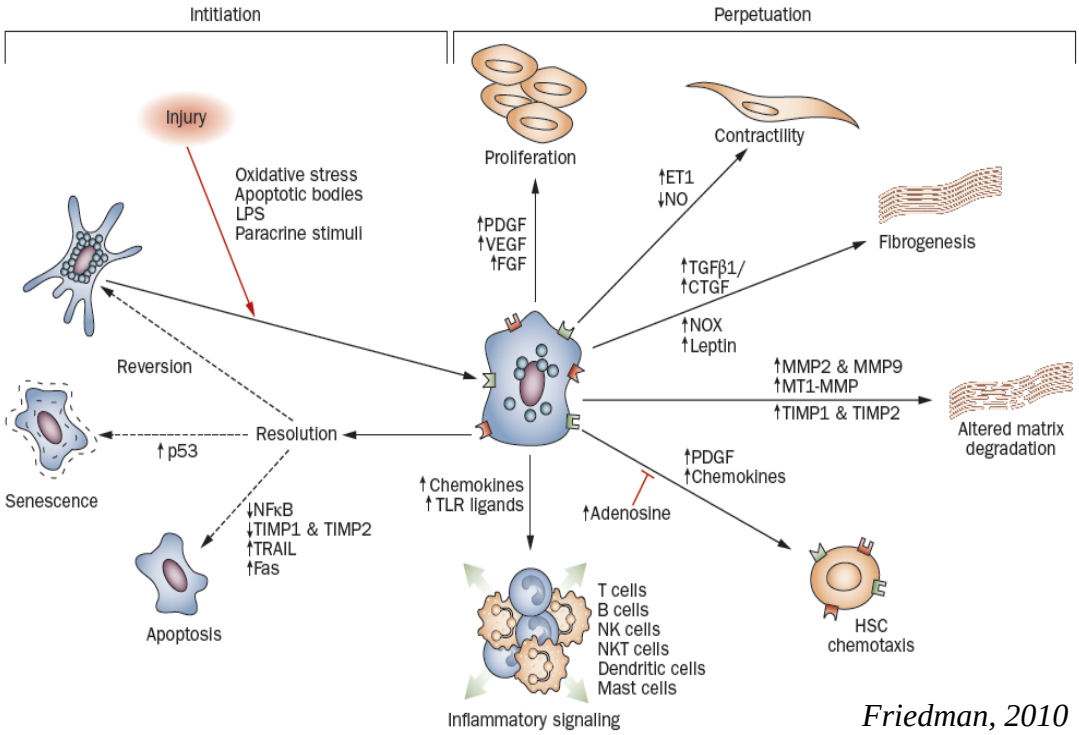

Figure 1.4: Molecular mechanisms involved in activation of hepatic stellate cells, fibrosis, and perpetuation into a tumorigenic form.

Interestingly, some research also indicates that hepatocytes and biliary epithelial cells may also contribute to myofibroblast formation during fibrosis of the liver. Hepatocytes and biliary epithelial cells of the liver may transdifferentiate into myofibroblasts through epithelial-to-mesenchymal transition (EMT, which will be explained later in detail) that may be mediated by TGF-β, Hedgehog and bone morphogenic protein 7 (BMP7), and contribute to ECM deposition and fibrosis [17].

Unlike the later stages of cirrhosis, fibrosis of the liver is a state that can be resolved, either through reversal of the fibroblastoid morphology by mesenchymal-to-epithelial transition (MET) [17], or through the elimination of fibrotic cells by senescence and apoptosis [13].

1.3.2 Senescence and Hepatocarcinogenesis

Senescence is a term that describes the process of becoming old, and cellular senescence is a phenomenon characterized by permanent cell cycle arrest [14]. Senescence can be identified by markers such as senescence-associated DNA-damage foci, senescence-asssociated heterochromatin foci, senescence-associated β-galactosidase (SABG) and $p16^{INK4A}$ [14].

Senescence can be inspected in three pathways; telomere-dependent senescence, oncogene-induced senescence, and ROS-induced senescence. All three of these pathways lead to senescence by triggering a DNA damage response in the cell (often induced by double strand breaks in the DNA), which activates ATM and ATR kinases, leading to the phosphorylation of p53 by CHK1 and CHK2 kinases. Phosphorylated p53 is released from MDM and stabilized, and can then induce senescence or apoptosis [14]. The form of senescence that is dependent on telomere shortening is also known as "replicative senescence" since telomere length acts as a cell-division counter in this case, as will be described in detail [14].

This cell cycle arrest, followed by apoptosis, may act as a barrier to the progression of HCC by acting as a means of eliminating fibrotic cells [13]. Senescent cells are observed at a ratio of 10% in normal liver, which is elevated to 84% in cirrhosis, and is reduced to 60% in HCC. These rates of senescence are mainly attributable to replicative senescence dependent on telomere shortening of hepatocytes. It was also observed that senescence-inducing proteins such as $p16^{INK4a}$ and $p21^{Cip1}$ accumulate in cirrhotic livers. Senescence-escape mechanisms such as telomerase reactivation, or mutations or epigenetic silencing events in senescence-inducing genes such as p53 and $p16^{INK4a}$ play important roles in the progression of HCC [14].

1.3.2.1 Telomere Shortening & Telomere-Dependent Senescence

Human chromosomes contain DNA-protein complexes named "telomeres" at the ends of each chromosome. Since DNA replication cannot initiate from the very ends of linear DNA, important genetic information would be lost by each replicative cycle without the availability of the TTAGGG telomere repeats at the ends of the

chromosomes. Therefore, the telomeres prevent genomic instability and the loss of essential genetic information by forming a cap at the ends of the chromosomes [14].

Majority of human somatic cells are incapable of synthesizing new telomeres due to the repression of telomerase reverse transcriptase (TERT) expression, therefore, telomeres become shorter with every cycle of cell division, acting as a "cell cycle counter" which helps determine when the cell should stop replicating. Shortened telomeres begin to lose their protected status, and such loss of telomere protection or any other form of telomere dysfunction leads to the formation of abnormal chromosomal end-to-end fusions through non-homologous end joining or homologous recombination pathways of DNA repair. The triggering of these DNA repair pathways indicate that open-ended telomere DNA is recognized as double strand breaks. This triggers a DNA damage response in the cell, which leads to senescence through the phosphorylation of p53, as previously mentioned, which activates $p21^{cip1}$, which is an inhibitor of Cyclin-dependent kinase 2 (CDK2). These events keep the tumor suppressing pRb protein in the active form, inhibiting E2F function and the expression of growth-promoting genes [14].

1.3.2.2 ROS-induced and Oncogene-induced Senescence

Reactive oxygen species (ROS) are mostly produced during cellular respiration at the mitochondria. *In vitro* methods of ROS induction such as mild H_2O_2 treatment and culturing under high O_2 conditions were shown to induce or aggravate senescence and cause reduced lifespans. ROS and oxidative stress may give rise to senesce through causing DNA damage or inducing changes in other signaling pathways [14].

Senescence has also been observed in response to the expression of well-studied oncogenes such as Ras, Raf, Myc, Cyclin E, Mek and Mos. In the case of Ras, expression of this oncogene was demonstrated to cause G1 arrest together with elevated levels of cell-cycle arrest associated proteins such as p53 and $p16^{INK4a}$ [14].

These two forms of senescence, like telomere-dependent replicative senescence, work primarily through DNA damage response pathways as well, but they can also induce other signals that lead to the activation of cyclin-dependent kinase inhibitors

such as $p16^{INK4a}$ and $p15^{INK4b}$ that inhibit CDK4 and CDK6 to keep the tumor suppressing pRb protein active [14]

1.3.3 Cirrhosis

As mentioned earlier, 80% of HCC cases originate as chronic liver disease and cirrhosis [14]. Although often mistakenly considered simply as an extended form of fibrosis, cirrhosis is, in fact, different from fibrosis in many ways. Cirrhosis is characterized by extensive inflammatory signaling, architectural disruption of the tissue due to excessive secretion of ECM proteins by myofibroblasts originating from stellate cells, aberrantly regenerating or senescent hepatocytes, nodule formation and vascular changes, and is often not reversible [13] [14].

1.4 Epithelial to Mesenchymal Transition and TGF-β

Epithelial cells of the adult human have a distinct apical-basal cell polarity, are often in layers of cells that are held together by cell-to-cell adhesion proteins such as E-cadherin, form a sheet on a basement membrane, and are immobile. Organs of the human body are often made up of organized, immobile epithelial cells that may mainly carry out secretory functions as in the cases of the liver and the pancreas. Mesenchymal cells, on the other hand, have very different phenotypes; they do not express E-cadherin, and are therefore not organized in layers having polarities, and they can migrate easily. Mesenchymal stem cells of the adult human reside in the bone marrow, and give rise to the highly mobile cells of the circulatory and lymphatic systems, as well as bone and cartilage tissues [18].

Epithelial to mesenchymal transition (EMT) is the reversible change of an epithelial cell into a mesenchymal or, in some cases, fibroblastoid phenotype. Epithelial cells that undergo EMT assume a more mesenchymal phenotype, losing their cell polarity and cell-to-cell adhesion characteristics and gaining the ability to transmigrate the

basement membrane and connective tissues to move into circulation, and becoming motile and invasive [15].

This switch from an epithelial to a mesenchymal phenotype is a normal part of embryonic development. It initially occurs during the gastrulation stage of the blastula, forming the mesoderm which gives rise to mesenchymal cells that contribute to extraembryonic tissues. Later in development, EMT contributes to the development of the circulatory, nervous and musculoskeletal systems [15].

In the adult, however, EMT usually occurs under pathophysiological circumstances such as chronic inflammation, wound healing response, and cancer progression. During wound healing, epithelial cells obtain reduced adhesiveness and increased migration capabilities during the process of producing new and intact epithelial layers. EMT is also observed during the non-regenerative repair attempt of an organ called fibrosis, which includes the dedifferentiation of epithelial cell types into a more fibroblastoid phenotype, contributing to the wound healing and inflammation response by secreting ECM proteins, and this event has been demonstrated to take part in liver fibrosis as well [15].

Transforming growth factor-β (TGF-β) is a cytokine that functions through Smad2/3 and Smad4 to control gene transcription and induce cellular effects such as growth inhibition, apoptosis, differentiation and extracellular matrix deposition [19]. The ultimate result of TGF-β signaling depends on the activities of other pathways in the cell, such as Ras signaling, and can have complex effects, as will be described.

1.4.1 Epithelial to Mesenchymal Transition and TGF-β in Liver Fibrosis

EMT has been demonstrated to participate significantly in liver fibrosis, with major contributions from the cytokine TGF-β. The first evidence that hepatocytes give rise to fibroblasts by going though EMT during liver fibrosis was provided by a study where EMT was induced in mouse hepatocytes by treatment with TGF-β1, and the hepatocytes were observed to change into fibroblast-specific-protein (FSP)-1 positive hepatic fibroblasts [20]. Another research study demonstrated that hepatocytes isolated from cirrhotic livers, which had been exposed to elevated levels of TGF-β *in*

vivo, had elongated, fibroblastoid-like phenotypes and expressed vimentin and collagen I [21]. Further research demonstrated that loss of epithelial phenotype in primary mouse hepatocytes in response to TGF-β treatment was associated with upregulation of SNAIL and consequent loss of E-cadherin expression[22] and that this also involved the activation of Smad2/3 signaling and collagen I synthesis [23].

Also very interestingly, it was demonstrated that EMT in primary murine hepatocytes was associated with FAK/Src dependent activation of the PI3K/Akt signaling, which causes resistance to apoptosis, as well as Erk1/2 signaling, which causes induction of EMT, demonstrating that EMT confers resistance against TGF-β-induced apoptosis [24]. This observation may be of particular interest to this study, as the Akt/Erk pathway is known to play key roles in cell survival under ER stress [25], for which the protein studied here, FAM134B may also play key roles, as will be discussed later in detail.

1.4.2 Epithelial to Mesenchymal Transition and TGF-β in the progression of Hepatocellular Carcinoma

TGF-β and EMT appear to play dual roles during the progression of hepatocellular carcinoma; in the healthy liver and during tumor initiation through fibrosis, TGF-β appears to induce cell cycle arrest, apoptosis and the development of a fibroblastoid-like phenotype, and at the neoplastic stage, TGF-β controls dedifferentiation and spreading of the neoplastic hepatocytes, contributing to the development of a poorly-differentiated state and metastatic behavior. [15]

Murine tumor models have demonstrated that a synergy between oncogenic Ras and TGF-β1 signaling causes EMT, malignant progression and metastasis, and that these are associated with loss of E-cadherin and the tight junction protein ZO-1, and activation of Smad2/3 leading to autocrine TGF-β signaling. Further studies showed that the induction phase of EMT requires crosstalk between TGF-β and MAPK, and that the maintenance phase depends on the activation of PI3K/Akt. EMT was also shown to be associated with increased platelet-derived growth factor (PDGF) signaling, independent of the genetic background of EMT, which was demonstrated

to cause migration and tumor progression. Interleukin-like EMT inducer (ILE1), which is a downstream target of TGF-β signaling, was shown to collaborate with oncogenic Ras to trigger the activation of STAT3, as well as the nuclear accumulation of β-catenin, via PDGF/ PDGF-R. [15]

Human studies were also supportive of the previous findings; studies with HCC cell lines revealed that elevated expression of the ECM protein laminin (Ln)-5 leads to the activation of Erk1/2, which is required for cell proliferation. In patient studies, 58% of HCC cases demonstrated reduced levels of E-cadherin. Loss of E-cadherin in HCC patients was reported to be accompanied by loss of β-catenin from cell borders and partial translocation to nucleus, as well as elevated levels of the ECM protein Laminin-5. Loss of E-cadherin also significantly correlated with intrahepatic metastasis and poor survival of patients. Also, expression of Twist, a negative regulator of E-cadherin expression, in non-metastatic HCC cells induced EMT and increased invasion. Also interestingly, viral proteins of HCV were also observed to render hepatocytes less sensitive to anti-proliferative effects of TGF-β. [15]

1.5 The Endoplasmic Reticulum

The endoplasmic reticulum (ER) is an organelle made up of a membrane-enclosed network of sacs, with central roles in protein and lipid synthesis, membrane biogenesis, xenobiotic detoxification, cellular calcium storage and the proper folding and modifying of proteins [26]. The ER membrane makes up more than half of the total membrane area of an animal cell, and is the production site of all transmembrane proteins in a cell, including those of the membrane-bound organelles and the plasma membrane. And the ER lumen is where almost all of the secretory proteins and proteins of the ER lumen itself, the Golgi apparatus and lysosomes are delivered for processing, folding and modifications. [27]

1.5.1 The Abundance and Functions of Rough and Smooth ER in Hepatocytes

Hepatocytes are the major providers of glucose and lipids to the entire human body, and they can produce millions of proteins per minute, possessing one of the highest rates of protein synthesis in the human body, and the overwhelming majority of these proteins are processed in the ER. [28]

The rough ER, which contains ribosomes on the cytosolic face, is mainly concerned with protein synthesis, and is abundant especially in cells that secrete proteins, for example, in hepatocytes that secrete proteins such as serum albumin or coagulation factors, or pancreatic β-cells that are responsible for insulin secretion. Most proteins synthesized in the rough ER are N-glycosylated and are destined for transport to the plasma membrane, Golgi apparatus, lysosomes or extracellular space, while proteins destined for the cytosol are often not glycosylated. Ca^{2+} dependent chaperones such as calnexin retain incompletely folded proteins in the ER until they are properly folded, depending on their N-glycosylation status. [27]

The smooth ER, on the other hand, lacks ribosomes, and is mainly concerned with lipid metabolism, carbohydrate metabolism, and detoxification. Smooth ER is very abundant in hepatocytes since these cells play key roles in lipid and carbohydrate metabolism, and are responsible for producing lipoprotein particles and detoxifying lipid-soluble drugs and metabolic byproducts. During detoxification of drugs or toxins such as phenobarbital or ethanol, the smooth ER of hepatocytes can double its surface area within a few days in order to be able to synthesize the unusually large amounts of detoxification enzymes required. [27]

Another fundamental responsibility of the ER is to store Ca^{2+}; the release and uptake of Ca^{2+} to and from the cytosol is involved in many rapid responses to extracellular signals, [27] and is involved in timing of the exocytosis of synthesized proteins, such as the release of insulin by pancreatic β-cells. The ER membrane contains an ATP-dependent channel that pumps Ca^{2+} from the cytosol into the ER lumen, generally named as sarco-endoplasmic reticulum Ca^{2+} ATPases (SERCA).

Calcium homeostasis is especially important for liver cells; Hotamisligil et al. have recently reported its implications in obesity by demonstrating that aberrant lipid

metabolism disrupts calcium homeostasis and causes liver endoplasmic reticulum stress in obesity [26]. Furthermore, recent research has shown that Ca^{2+} gradients are also important for the coating and uncoating of transport vesicles that are trafficked between the ER and the Golgi apparatus [29].

1.5.2 Endoplasmic Reticulum Stress and the Unfolded Protein Response

A sudden high demand of protein synthesis, inducers of oxidative stress, or some other disruption of ER homeostasis can cause the accumulation of misfolded proteins in the ER, and this triggers the unfolded protein response (UPR). The accumulation of unfolded proteins in the ER is sensed by the binding immunoglobulin protein/glucose-regulated protein 78 (BiP/GRP78). Upon being sequestered by misfolded proteins, BiP/GRP78 dissociates from the three known ER-membrane transducers, inositol requiring 1α (IRE1α), PKR-like ER kinase (PERK), and activating transcription factor 6α (ATF6α), allowing their activation. These three transducers initiate a response that aims to alleviate ER stress by reducing the load of new peptides entering the ER, increasing the folding capacity of the ER and degrading misfolded proteins. [30]

PERK phosphorylates eukaryotic initiation factor 2 alpha (eIF2α), which attenuates global mRNA translation, aiming to alleviate some of the peptide burden on the ER. PERK also selectively increases the translation of ATF4, which is a transcription factor that induces the expression of chaperones, amino acid transporters, antioxidant stress response genes, ER-associated degradation (ERAD) proteins and C/EBP homologous protein (CHOP), which can cause apoptosis if ER stress persists. [30]

IRE1α has kinase and RNAse activities; its autophosphorylation activates the RNase activity to splice X-box binding protein 1 (XBP1) mRNA, allowing the production of the active transcription factor sXBP1. sXBP1 upregulates ER chaperones, ERAD proteins, and CHOP. IRE1a activation also facilitates mRNA degradation and translation attenuation, in collaboration with PERK. IRE1α also recruits and activates C-jun N-terminal kinase (JNK), which is a stress kinase that can mediate apoptosis under persistent ER stress. [30]

ATF6α released from BiP/GRP78 transports to the Golgi apparatus, where it is cleaved and activated by intramembrane proteolysis. The activated transcription factor ATF6α heterodimerizes with and activates sXBP1 to induce the transcription of chaperones, ERAD proteins and CHOP. [30]

Unresolved ER stress results in apoptosis through mechanisms involving CHOP, JNK, Bcl-2 family proteins, calcium and redox homeostasis, and caspase activation [30]. For instance, apoptosis induced by ER stress has been shown to involve disruption of calcium homeostasis and protein accumulation, which leads to the calpain-mediated activation of caspase-12, which is localized to the ER [31]. In fact, disruption of calcium homeostasis appears to be very important for the link between ER stress and apoptosis. Overexpression of the anti-apoptotic protein Bcl-2 was shown to reduce free ER calcium and cell death, while reduction of the pro-apoptotic proteins Bak and Bax resulted in lower free ER calcium and reduced sensitivity to apoptotic stimuli such as hydrogen peroxide treatment. [30]

1.5.3 Endoplasmic Reticulum Stress, Obesity and Liver Disease

Hepatocytes, pancreatic exocrine cells and adipoctyes constitute a triad of cells that have very important metabolic functions, have high protein synthesis rates, and are therefore very sensitive to ER stress brought on by disruptions of metabolic homeostasis, such as excess nutrients, insulin peaks, and obesity. [28]

Obesity is a risk factor for non-alcoholic fatty liver disease, type 2 diabetes, and hepatocellular carcinoma, which are all interconnected. In mouse models, obesity has been demonstrated to induce ER stress in liver and adipose tissues of mice. A high demand on adipocytes to store more lipids than they can handle causes production of reactive oxygen species (ROS), inflammation, ER stress, apoptosis, and increased fatty acid (FA) release. The excess circulating FAs are taken up by the liver, and cause a lipotoxicity that alters glucose utilization and insulin action, and results in steatosis of hepatocytes. In the livers of obese mice, ATF6α expression was observed to be reduced, and its reconstitution was observed to improve glucose homeostasis. [32]

The UPR influences metabolic processes in complex ways, as described in Figure 1.5. In hepatocytes, XBP1 induces increased FA synthesis, while activation of ATF6α inhibits the induction of lipogenic genes by sterol regulatory element-binding protein (SREBP), however, mouse models lacking hepatic ATF6α showed increased steatosis regardless of the reduced levels of lipogenesis, indicating that more complex mechanisms were involved. ATF6α also has an inhibitory effect on gluconeogenesis, modulating the activity of the key transcriptional regulator cAMP-response element binding protein (CREB). [32] Also interestingly, liver samples

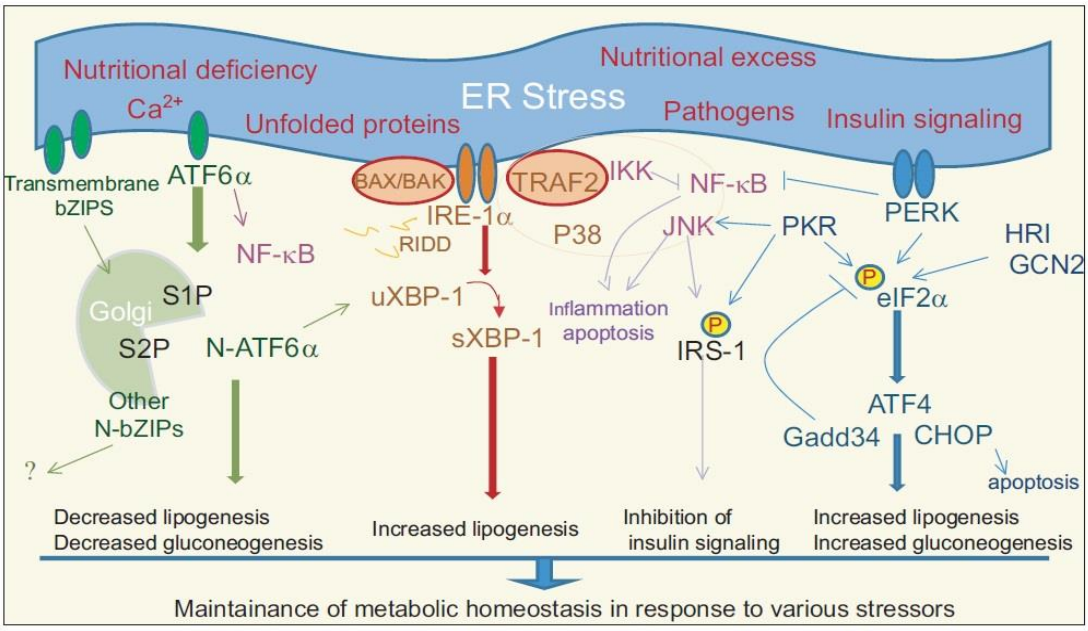

Figure 1.5: Metabolic causes and consequences of ER stress and the UPR. *Hotamisligil, 2010* [32]

from patients with non-alcoholic fatty liver disease have demonstrated elevated BiP expression and eIF2α phosphorylation. Genetic modulation studies on the pathways involving eIF2α phosphorylation, IRE1α/XBP1, and ER protein translocation have linked ER stress and hepatocyte steatosis. [30] Also, CHOP has been implicated in hepatocyte death as a mediator of decreased gene expression under severe ER stress [32]

Several damaging agents that disrupt ER homeostasis, such as drugs, alcohol, lipids, and HBV and HCV have been shown to cause ER dysfunction through mediators such as ROS that cause oxidative stress, altered membrane lipid composition, and

formation of protein aggregates, which can either be resolved or have more serious consequences such as inflammation, steatosis, and apoptosis of hepatocytes [30].

1.5.4 ER Stress, Epithelial to Mesenchymal Transition and Src Kinase

It is also important to note that sustained ER stress and EMT appear to be closely related. Recent studies on thyroid and alveolar epithelial cells have demonstrated that induction of ER stress by chemical inducers such as thapsigargin and tunicamycin resulted in epithelial to mesenchymal transition as demonstrated by loss of epithelial markers such as E-cadherin, and increase of mesenchymal markers such as α–smooth muscle actin (α-SMA), as well as morphological changes. Both studies also utilized the PP2 inhibitor of Src-family kinases to demonstrate that the induction of dedifferentiation and EMT by ER stress was mediated by the Src pathway. [33] [34] Src is a non-receptor proto-oncogene tyrosine protein kinase that is hyperactive in many cancers and is a drug target for tyrosine kinase inhibitors such as dasatinib.

1.6 FAM134B in Literature

A review article published in EMBO Reports in 2010, titled "Further assembly required: construction and dynamics of the endoplasmic reticulum network" draws attention to the family with sequence similarity 134 (FAM134) family of proteins FAM134A, FAM134B and FAM134C, and points out that these proteins may constitute a new family of organelle-shaping proteins since each of the FAM134 proteins have a pair of long hydrophobic segments similar to those found in reticulons and DP1/REEPs/Yop1. [35] Reticulons are a class of membrane proteins shaping the tubular endoplasmic reticulum, primarily functioning in promoting membrane curvature. Reticulons interact with DP1/Yop1p, another tubular ER membrane protein, and their deficiency disrupts tubular ER. [36]

A 2009 publication in Nature Genetics by Kurth et al. established that loss-of-function mutations in FAM134B cause hereditary sensory and autonomic neuropathy

type II (HSANII), which involves severe mutilations due to diminished sensory perception and compromised regulation of involuntary functions of the body. The FAM134B protein was shown to co-localize with the cis-Golgi protein giantin, and was therefore defined as a Golgi protein. Using primary dorsal root ganglion neurons, it was revealed that knockdown of FAM134B results in a ~40% reduction in the size of the cis-Golgi compartment as well as apoptosis. Analyses on multiple adult murine tissues showed that FAM134B was most highly expressed in the testis, followed by the dorsal root ganglion, while the liver had much lower expression levels. [37]

In 2007, Tang et al. published a study entitled "Oncogenic properties of a novel gene JK-1 located in chromosome 5p and its overexpression in human esophageal squamous cell carcinoma." JK-1 is an alias for FAM134B isoform 2, and this study established that elevated levels of JK-1 is associated with esophageal squamous cell carcinoma (ESCC) and can transform normal cells. They observed that 30% (9/30) of ESCC tumors , and 69% (9/13) of ESCC cell lines had elevated levels of JK-1. They also demonstrated that overexpression of JK-1 promoted anchorage dependent and anchorage independent proliferation of benign NIH3T3 and HEK293 cells. Moreover, subcutaneous injections of NIH3T3 cells overexpressing JK-1 formed sarcomas in all three mice. [38]

Another interesting publication from 2011 assembled gene expression data from pluripotent stem cells and non-pluripotent cells of the mouse, and identified FAM134B as a biomarker of pluripotent stem cells in mice, and suggested that FAM134B may constitute a missing link between pluripotency and some unidentified surface markers processed by the Golgi apparatus. However, it is not clear from this paper whether FAM134B is overexpressed or underexpressed in pluripotent cells [39]

FAM13B initially caught attention in our laboratory as a possible senescence-associated gene, as its levels were elevated in senescent Huh7 clones compared to parental and immortal Huh7 clones. Further studies implicated that FAM134B is not a cause but a result of senescence. It was also identified to co-localize with the ER protein Calnexin. FAM134B protein levels were also shown to be elevated in the

more mesenchymal-like, poorly-differentiated HCC cell lines compared to the more epithelial-like, well-differentiated ones, and we hypothesized that this could be associated with the elevated ER stress status of the more mesenchymal-like cell lines. [40][41] (Nilgün Taşdemir, Mustafa Yılmaz and Mehmet Öztürk, unpublished data)

2. OBJECTIVES AND RATIONALE

Hepatocellular carcinoma constitutes 80% of liver cancers, which is the cancer type with the second poorest survival rates worldwide [3]. Risk factors for hepatocellular carcinoma include alcohol consumption and HBV or HCV infections, in addition to obesity, non-alcoholic fatty liver disease and diabetes, all of which appear to have devastating impacts on the endoplasmic reticulum and the cell, as described in the introductory section.

FAM134B initially caught attention in our lab in comparative analyses, having elevated levels in senescent Huh7 clones compared to parental and immortal Huh7 clones. Further analyses showed that it may be localized on the ER, and that its levels are elevated in the more mesenchymal-like HCC cell lines, which also have elevated ER stress status. [40]

An EMBO report published in 2010 drew attention to the FAM134B protein as a possible organelle shaping, reticulon-like protein of unknown function that is yet to be placed in the ER network [35]. And a 2009 publication in Nature identified FAM134B as a cis-Golgi protein for which loss-off function mutations cause neuropathy [37].

This research aims to identify the function of the FAM134B protein, with special focus on its role in hepatocellular carcinoma.

3. MATERIALS AND METHODS

3.1 MATERIALS

3.1.1 General Laboratory Reagents and Kits

General laboratory reagents, chemicals and kits utilized during the course of this thesis work were all laboratory-grade commercial products purchased from major companies. Tunicamycin, ready-made Bradford reagent, Bovine Serum Albumin (BSA), haematoxylene dye, agarose, ethanol and methanol were bought from Sigma-Aldrich (St. Louis, MO, USA). Sulforhodamine B (SRB) dye was in powder form and also obtained from Sigma-Aldrich (St. Louis, MO, USA). Thapsigargin was purchased from Santa Cruz Biotechnology Inc. (Santa Cruz, CA, USA). TGF-β1 was purchased from R&D Systems (Minneapolis, USA). Nucleospin RNA II total RNA isolation kit was purchased from Macherey-Nagel (Duren, Germany). TRIsure RNA isolation reagent used for tissues was purchased from Bioline (Taunton, USA). Ponceau dye and cell culture grade dimethyl sulfoxide (DMSO) were obtained from Applied Biochemia (Darmstadt, Germany). ECL prime detection reagent and Nitro-cellulose western blot membranes were purchased from Amersham GE Lifesciences (Pittsburgh, PA, USA). For immunoperoxidase staining, the DAKO EnVision+ system was used, which included blocking solution and secondary antibody mix (Glostrup, Denmark).

3.1.2 Cell Culture Solutions and Materials

Dulbecco's modified Eagle's medium (DMEM) and Roswell Park Memorial Institute (RPMI) cell culture mediums, fetal bovine serum (FBS), penicillin/streptomycin antibiotics, L-glutamine and trypsin-EDTA were purchased from GIBCO (Invitrogen, Carlsbad, CA, USA). The plastic items used in cell culture such as cell

culture plates, flasks and serological pipettes were obtained from Corning Life Sciences Inc. (USA).

3.1.3 Electrophoresis Apparatus

The SDS-PAGE gel electrophoresis equipment, including the tanks, the gel preparation glasses, power supplies and other plastic materials were purchased from BIO-RAD Laboratories (CA, USA). Agarose gel electrophoresis apparatus and NanoDrop spectrophotometry apparatus to measure nucleic acid concentration were obtained from Thermo Scientific (Wilmington, USA). Protein concentration was determined using Bradford reagent which was measured using the spectrophotometer Beckman Du640 from Beckman Instruments Inc. (CA, USA).

3.1.4 cDNA Synthesis and Polymerase Chain Reaction Reagents

All reagents required for cDNA synthesis from total mRNA and semi-quantitative polymerase chain reaction (PCR) were obtained from Fermentas (MBI Fermentas, Germany), including RevertAid First strand cDNA synthesis kit, Taq DNA polymerase, 10X Taq DNA polymerase Buffer (+$(NH_4)_2SO_4$,–$MgCl_2$), 2mM dNTPs, 25mM $MgCl_2$ and DNA molecular weight ladders.

3.1.5 Primers

Primers were ordered from Sentromer (Istanbul, Turkey).

Primer	**Sequence**	**Tm**
mmFAM134B isoform 1 For.	AGC TCC TGA GCT GGA AGA GG	61
mmFAM134B isoform 1 Rev.	TCA TGA CGG AAA TGA GGT GA	55
mmFAM134B isoform 2 For.	GCT GTG GAC CAG GCA GAA G	61
mmFAM134B isoform 2 Rev.	AAA TTC ATC CAT GAT TCT GCA A	53
mmXBP-1spl.unspl. For.	AGT TAA GAA CAC GCT TGG GAA T	57

mmXBP-1 spl.unspl. Rev.	AAG ATG TTC TGG GGA GGT GAC	60
hFAM134B isoform 1 For.	CAAGAGGTGCACAGTTGTGGAGAA	58
hFAM134B isoform 1 Rev.	GCAACCGTGAGGCTAATCTTAGGA	58
hFAM134B isoform 2 For.	CTCGAGAAGCTTATGCCTGAAGGTGAA GACTT	58
hFAM134B isoform 2 Rev.	GCAACCGTGAGGCTAATCTTAGGA	58
hXBP-1 For.	TTACGAGAGAAAACTCATGGCC	58
hXBP-1 Rev.	GGGTCCAAGTTGTCCAGAATGC	62
hGAPDH For.	GGCTGAGAACGGGAAGCTTGTCAT	60
hGAPDH Rev.	CAGCCTTCTCCATGGTGGTGAAGA	60
hVimentin For.	CGTCACCTTCGTGAATACCA	60
hVimentin Rev.	CCAGAGGGAGTGAATCCAGA	60

Table 3-1: Primer sequences and Tm values.

3.1.6 Antibodies

Antibody	**Company and Catalog Number**	**Dilution**
FAM134B	Sigma, HPA026906	1:2500
Phospho-eIF2α	Invitrogen, 44728G	1:1000
Vimentin	Dako, M7020	1:500
Calnexin	Sigma, C4731	1:5000
α-tubulin	Calbiochem, CP06	1:4000
actin	Santa Cruz, sc-1616-R	1:5000
anti-mouse-HRP	Sigma, A0168	1:5000
anti-rabbit-HRP	Sigma, 6154	1:5000

Table 3-2: Antibodies, source companies and dilutions used.

3.2 SOLUTIONS AND MEDIA

3.2.1 General solutions

10X Phosphate Buffered Saline (PBS)	80g NaCl, 2g KCl, 14.4g Na_2HPO_4, 2.4g KH_2PO_4 in 1 liter ddH_2O
50X Tris Acetate EDTA (TAE)	242 g Tris base, 57.1 ml glacial acetic acid, 18.6 EDTA in 1 liter ddH_20
6X DNA Loading Dye	10mM Tris-HCl (pH 7.6), 0.03% bromophenol blue, 0.03% xylene cyanol, 60% glycerol, 60mM EDTA (0.5M pH8.0)
Ethidium Bromide	10 mg/ml dissolved in ddH_2O (stock) 1:10.000 working dilution (1µl per 10ml of gel)

3.2.2 Tissue culture solutions

Complete Medium	500ml DMEM/RPMI medium, 10% filtered and inactivated fetal bovine serum, 1% penicillin / streptomycin, 1% non-essential amino acids, 1% L-glutamine. Stored at 4℃
Freezing Medium	20% FBS and 7% DMSO added to complete medium
10X Phosphate buffered saline (PBS)	80g NaCl, 2g KCl, 14.4g Na_2HPO_4, 2.4g KH_2PO_4 in 1 liter ddH_2O, working dilution: 1X, autoclaved and stored at 4℃

3.2.3 RIPA Lysis Buffer for Protein Extraction

The RIPA lysis buffer for protein extraction was prepared in advance excluding the protease inhibitor and NaF and $NaVO_4$ which serve as phosphatase inhibitors, and stored in 4℃ as stock. Protease inhibitor and the phosphatase inhibitors were added fresh before use, and this solution could only be stored up to 3 months at -20℃.

	Stock Concentration	**Final Concentration**	**For 1ml**	**For 50ml stock**
ddH_2O			730µl	36.5ml
NaCl	2M	150mM	75 µl	3.750ml
NP-40/TritonX		1%	10 µl	500 µl
Sodium DOC	10%	0.5%	50 µl	2.500ml
SDS	10%	0.1%	10 µl	500 µl
Tris-HCl pH8	2M	50mM	25 µl	1.250ml
Protease Inhibitor	25X	1X	40 µl	* added fresh
NaF	1M	50mM	50 µl	* added fresh
$NaVO_4$	100mM	1mM	10 µl	* added fresh

Table 3-3: RIPA lysis buffer ingredients and recipe.

3.2.4 Sodium Deodecyl Sulphate–Polyacrylamide Gel Electrophoresis (SDS-PAGE) Gels and Solutions for Western Blotting

10% Running Gel (7mls recipe for 1 gel)	2.66ml ddH_2O, 2.38ml 30% Acrylamide Mix, 1.82ml 1.5M Tris-HCl pH8.8, 70 µl 10% SDS, 70µl 10% Ammonium Per Sulfate, 2.8µl TEMED
5% Stacking Gel (3mls recipe for 1 gel)	2.1ml ddH_2O, 500µl 30% Acrylamide Mix, 380µl 1M Tris-HCl pH6.8, 30µl 10% SDS, 30µl 10% Ammonium Per Sulfate, 3µl TEMED
10X SDS Running buffer	144g glycine, 30g Tris were dissolved in dH_2O, 50ml 10% SDS was added, and the volume was completed to 1 L. Working solution is 1X.
10X Transfer buffer	72g glycine, 58g Tris were dissolved in dH_2O, 2ml 10% SDS was added, and the volume was completed to 1 L. Working solution is 1X containing 15-20% EtOH
Protein Loading Dye	5% 14.3M β-mercaptoethanol was added to protein loading dye before use
10X Tris buffered saline (TBS)	12.19g trisma base and 87.76g NaCl were dissolved in 1 L of ddH_2O, and pH is adjusted to 8.
TBS-T (0.2%)	10X TBS diluted to 1X working solution, and 2:1000 Tween added
Coomassie brilliant blue solution	100mg coomassie brilliant blue G-250, 50ml 95% ethanol, 100ml 85% phosphoric acid. Filtered using whatman paper
Ponceau solution	0.1% (w/v) Ponceau S and 5% (v/v) acetic acid in ddH_2O
Blocking solution	5% (w/v) non-fat dry milk or 5% (w/v) Bovine Serum Albumin (BSA) dissolved in TBS-T

3.2.5 Immunoperoxidase staining solutions

Fixation	1:1 Acetone:Methanol
Washing solution	PBS-T; 0.2% Tween 20 in 1X PBS
Antibody dissolved in	2% FBS in 0.2% PBS-T

3.2.6 Sulforhodamine B (SRB) staining solutions

10% TCA	10% (wt/vol) trichloroacetic acid in ddH_2O
10X (4%) SRB Stock	4g SRB powder dissolved in 100ml 1% acetic acid, stored at room temperature, working dilution is 1X
Tris Base Solution	10mM Tris base solution was prepared with no pH adjustment
1% acetic acid	1% (vol/vol) acetic acid in ddH_2O

3.3 METHODS

3.3.1 Mouse Experiments

3.3.1.1 Tunicamycin Treatment of the Mice

14 C57 black 6 (C57BL/6) laboratory mice of around 20g of body weight, fed with normal diets were used for these experiments. The 14 mice were separated into 2 groups of 7; one was the sucrose control group, the other was the tunicamycin treatment group. The tunicamycin treated group was injected with 1ug/g body weight of tunicamycin; the tunicamycin solution was prepared at a concentration of

100ug/ml, therefore, a mouse of 20grams body weight received an injection of 200ul. The tunicamycin was dissolved in a 150mM sucrose solution which was prepared in physiological saline. The sucrose control group was injected with 150mM sucrose solution at a volume of 10ul/g body weight, again equaling a 200µl injection for a 20g mouse. The mice were maintained for 8 hours under normal conditions during the course of the 8 hours of tunicamycin treatment.

3.3.1.2 Collection of Liver Tissue from Mice

The mice were sacrificed and liver tissues were collected. Each liver sample was divided into 3 sections; one for RNA isolation, one for protein isolation, and one for immunohistochemistry (IHC). The sections reserved for RNA and protein isolation were immediately frozen in liquid nitrogen and stored at -80℃. The sections reserved for IHC were fixed in 4% formaldehyde for one day and then paraffinated and stained with Hematoxylin and eosin method by the Animal Facility technicians.

3.3.1.3 RNA Isolation from Mice Liver Tissues

The TRIzol or TRIsure method was used to isolate RNA from tissues; all steps were performed on ice in the fume hood. A section of 50-100mg of each tissue was put in a round bottom tube containing 1.5mls of TRIsure, the mixture was homogenized using a sterilized homogenizer, which was cleaned with ddH_2O and sterilized with ethanol between each sample. The contents were pipeted to a 2ml eppendorf, and 300µl chloroform was added, and they were mixed vigorously by shaking up and down for 15 seconds. After 3 minutes at room temperature, they were centrifuged at 15000rpm for 15 minutes, at 4℃. The clear top layer of supernatant was taken into a new eppendorf without touching the white interphase that contained cell waste. 750µl isopropanol was added and mixed slowly. After 10 minutes at room temperature, the mix was centrifuged at 14000rpm for 10 minutes at 4 ℃. The isopropanol was removed carefully, keeping the RNA pellet. The RNA pellet was washed twice with ethanol, for 8 minutes at 8000rpm at 4℃. The pellet was then dried under the fume hood and dissolved in RNAse DNAse free water, and stored at -80℃.

3.3.1.4 Protein Isolation from Mice Liver Tissues

The following steps were performed on ice. A 50-100ug section of each tissue was homogenized in 500µl RIPA buffer, then kept on ice and vortexed every 5 minutes for 30 seconds. The samples were then sonicated and centrifuged at 11000rpm for 30 minutes, at 4℃. The supernatants were taken into new eppendorfs, and the centrifugation step was repeated two more times in order to get rid of the lipids that stick to the eppendorf during centrifugation. The samples were stored at -80℃.

3.3.2 Tissue culture methods

3.3.2.1 Culturing of HCC Cell Lines

Huh-7, PLC, Hep40 and Hep3B cell lines were cultured in complete DMEM medium while Snu387, Snu398, Snu449, and Snu475 were cultured in complete RPMI medium. Complete mediums contained 10% inactivated and filtered fetal bovine serum, 1% penicillin/streptomycin antibiotics, 1% L-glutamine, and 1% non-essential amino acids. The cells were maintained in incubators at 37°C with filtered air circulation containing 5% carbon dioxide. Cells were passaged before reaching full confluency in order to prevent cell cycle arrests. All liquids such as mediums and PBS that come in contact with the cells were heated to 37℃ in the water bath before use, and all equipment and solutions utilized were sterile.

3.3.2.2 Cell Passaging

In order to passage the cells, the medium was aspirated and the cells were washed once with PBS. The cells were then trypsinized using 500-2000µl of trypsin depending on size of the plate or flask, and incubated at 37℃ for 1-2 minutes to activate the trypsin and detach the cells. The cells were collected from the plates using complete medium, and pipeted well to dissociate any clumps. The required amount of cells was transferred to a new dish in fresh medium, the amount of which is determined according to the dish or flask used.

3.3.2.3 Cell Thawing

In order to start a new cell culture from a cryopreserved stock in liquid nitrogen or -80℃ freezer, the vial was first only briefly kept on ice or at -20℃. It was then quickly thawed in the 37℃ water bath for a few minutes, and transferred to a 15ml falcon which contained 10mls of medium warmed to 37℃, and mixed well. The falcon was then centrifuged at 1500 rpm for 4 minutes and the medium was aspirated to remove any DMSO from cryopreservation. The dish or flask size to be used was determined according to the size of the cell pellet. The pellet was dissolved in new complete medium and transferred to a new dish or flask, and was dispersed well by moving the plate side to side and back and forth. The cells were then incubated at 37℃ and 5% carbon dioxide, and checked regularly to change the medium or be passaged before reaching confluency.

3.3.2.4 Cell Cryopreservation

Cells were cryopreserved when they reach 70-80% confluency since cells that are too confluent can go into growth arrest. Cells were washed with PBS, trypsinized, collected into falcons and centrifuged at 1500 rpm for 4 minutes, and medium was aspirated. The cell pellet was then resuspended in freezing medium with 20% FBS and 7% DMSO and pipeted well to ensure there were no clumps. The number of vials to preserve depended on pellet size, and each vial was prepared to contain around enough cells to fill a 10mm dish, resuspended in 1.5-2mls of freezing medium. The vials were initially cooled for 1hour at -20°C and then transferred to -80°C and liquid nitrogen for preservation.

3.3.2.5 Cell Treatments

The cells were plated in the suiting plates, dishes or flasks in specific numbers that aimed the control cells to reach a confluency of 80-90% by the end of the total treatment period. 24 hours after seeding, the mediums were changed to contain the desired concentration of the chemical in complete medium, prepared fresh. Mediums used for the control samples contained the solvent of the drug, such as DMSO.

3.3.3 mRNA Expression Analyses

3.3.3.1 Total RNA Extraction from Cells

The cells were collected by trypsinization, and after the first centrifuge and removing the medium, the pellet was washed a second time with cold PBS and centrifugation. The pellet could be stored at -80°C. Total RNA isolation was carried out using the protocol provided with the NucleoSpin RNA II Kit (MN Macherey-Nagel, Duren, Germany).

3.3.3.2 cDNA synthesis (Reverse Transcription)

RNA concentrations were determined using NanoDrop and equal amount of total RNA from each sample was used, which was 2-4ug. The Fermentas RevertAid cDNA synthesis Kit (MBI Fermentas, Germany) was utilized to carry out cDNA synthesis in a total volume of 20ul, as described by the protocol provided with the kit, using the thermocycler machine. The initial step of incubating the RNAs only with Oligo(dT) primers ensured that only the mRNAs with PolyA tails can be reverse transcribed. Then dNTPs, Ribonuclease inhibitor, reaction buffer, and finally, RevertAid MuLV Reverse Transcriptase were added to complete the reverse transcription. Reverse transcriptase negative controls for each sample were also prepared to ensure there was no genomic DNA contamination, which could be detected in the PCR products as a band of a different size due to introns.

3.3.3.3 Primer Design for Semi-Quantitative RT-PCR

Primers were designed to be on different exons so that a PCR product from genomic DNA would have a different size since it contained an intron. Also, specifity for the desired mRNA was double-checked in BLAST, and primers yielding homo- or hetero-dimers were eliminated using predictions on the online IDT Oligo Analyzer tool. The forward and reverse primer pairs were also adjusted to have similar melting temperatures, and low GC contents.

3.3.3.4 Polymerase Chain Reaction

GAPDH was always used as a loading control. Optimizations on melting temperature were made using Gradient PCR when needed. The total volumes of the reactions were 25ul, and 10µl reactions were used for optimizations to spare cDNA. The core reaction was;

Initialization	5 minutes at 95°C	
Denaturation	30 seconds at 95°C	20-30-32 cycles
Annealing	30 seconds at 58-60°C	
Elongation	30 seconds at 72°C	
Final Extention	10 minutes at 72°C	
Final Hold	4°C	

3.3.3.5 Agarose Gel Electrophoresis

The gel was prepared to contain 2-3% agarose and ethidium bromide in 1X TAE. The separation of the unspliced and spliced XBP bands could best be visualized with a 3% gel. PCR products were mixed with 6X loading dye and loaded very carefully to ensure correct comparison. The gels were run at 100-130V voltage to get sharp bands, with 50bp ladders, and visualized under UV light.

3.3.4 Protein Level Analyses

3.3.4.1 Total Protein Extraction from Cultured Cells

The cells were collected via trypsinization or scraping, and washed with cold PBS. All PBS was removed with a second centrifugation step. The pellets were resuspended in 30-25µl of RIPA Lysis Buffer depending on pellet size. They were kept on ice and vortexed every 5 minutes for 30 minutes. The samples were then sonicated and boiled for 3 minutes to separate DNA. The samples were then

centrifuged at 15000rpm for 1 hour at 4°C. Supernatants were collected to new eppendorfs and protein concentrations were determined using the Bradford method, often in triplicates of different concentrations to ensure equal loading. The absorbances were measured at 595nm in the spectrophotometer, and the concentrations were calculated from the absorbance values using the formula of the reference BSA graph obtained by absorbance values of BSA solutions of known concentrations.

3.3.4.2 Western blotting

After determining the protein concentration of each sample, the volume required for 20-30ug of protein from each sample was calculated, and an equal total protein amount among all samples was ensured. Samples were prepared for loading with the addition of a 5X SDS loading dye containing 5% β-mercaptoethanol as a denaturing agent and water to complete to same total amount of around 25ul. Before loading, these mixtures were boiled at 100°C for 10 minutes for denaturing.

The gels, running buffers and transfer buffers were prepared as described in the recipes in the materials section. During running and transfer, the buffers were kept cool by placing a cooler into the tank. Running was performed at a fixed ampere, which was about 20mA per gel, and lasted 1-2 hours. The sponges, whatman papers and nitrocellulose membranes were wetted in transfer buffer prior to setting up the wet transfer. The transfer was performed at 100V for 60 minutes. After visualization of the total protein with Ponceau dye to ensure equal loading, the membranes were shaken slowly at room temperature in blocking solution for 1 hour. Primary antibody incubations were done at 4°C overnight on a slow shaker, secondary antibody incubations were done for 40-60 minutes at room temperature on slow shaker, and washes were done on vigorous shaking with TBS-T for 5-15-5 minutes.

The bands were visualized using ECL prime western blot detection kit (Amersham, Buckinghamshire, UK) prepared 1:1 and developed for 5 minutes. Exposure times to X-ray film varied between 10 seconds to 10 minutes, depending on antibody strengths.

3.3.4.3 Immunoperoxidase Staining

Before plating the cells on 6-well plates, an autoclave-sterilized coverslip was placed at the bottom of each well. After plating the cells in equal amounts, the plates were shaken side to side and back and forth to ensure equal dispersion. The cells were grown 24 hours and then washed slowly with cold PBS. They were then fixed for 5 minutes with ice-cold 1:1 methanol:acetone mixture, which also allowed permeabilization of the membranes.

The cells were blocked with Lab Vision Blocking Solution provided with the DAKO kit, or 5% BSA in PBS for 10 minutes. Primary antibody was prepared in 3% BSA in PBS, and incubated 2 hours at room temperature, ensuring the slides cannot go dry. 50µl of primary antibody mixture was enough for one coverslip. The slides were washed 3 times for 3 minutes in PBS-T and excess was dried. As a secondary antibody, the slides were incubated with Lab Vision Biotinylated Goat Anti-Polyvalent for 10 minutes, lid closed. The slides were washed 3 times for 3 minutes in PBS-T and excess was dried and then incubated with Lab Vision Streptavidin Peroxidase for 10 min, lid closed. The slides were washed 3 times and dried as before. DAKO DAB was prepared 1 drop in 1000ul, vortexed, and kept in dark. Each sample was incubated with DAB for 5 minutes, and washed with plenty of ddH_2O. Hematoxylene was filtered, vortexed and poured in a tissue staining jar, and slides were kept in Hematoxylene for 30 seconds, and then washed thoroughly under running tap water. Excess water was dried off and coverslips were mounted onto microscopic slides using DAKO Fluorescent Mounting Medium and photographed.

3.3.5 Stable Knockdown with shRNA

The stable knockdowns of FAM134B expression in Snu449 cells were performed by previous lab members (P. Telkoparan, H. Alotaibi, N. Tasdemir, of M. Ozturk Lab, personal communication) using pGIPZ plasmids which conferred puromycin resistance to the cells. Puromycin resistance was utilized to select and proliferate single colonies that expressed the plasmid carrying the shRNA construct for

FAM134B. Stable cell lines were maintained in puromycin-containing medium, and knockdowns were confirmed using western blot and reverse transcription PCR.

3.3.6 Wound Healing / Scratch Assay

The cells were plated in complete medium on 6-well plates in numbers enough to reach 100% confluency after 24hours, which was about 400.000 for the stable Snu449 cell lines. After 24 hours, when the cells have become confluent, the wells were washed gently with PBS, and scratches were introduced using a micropipette tip. Wells were washed twice more with PBS, and new medium with 0.05% FBS was put on the wells, to prevent cell division. To observe migratory behavior, the cells were photographed at the same region at 0 hours, 24 hours and 48 hours.

3.3.7 Sulforhodamine B (SRB) Colorimetric Assay

A 96well plate was prepared for an SRB assay by labeling and filling the outer wells with 200µl PBS to prevent evaporation of samples. The cells were counted and prepared in the right concentration in order to be plated at equal numbers (4000 for Snu449 cells) in 100µl of medium. After 24 hours, the drugs were prepared in increasing concentrations, as 2X in 100ul; when added onto the previous 100µl medium on the cells, the concentration becomes the desired 1X concentration. The samples were all prepared in triplicates.

After 72 hours of incubation with the drugs, the cells were fixed with 10% TCA for 60 minutes at 4°C, and then washed with dH_2O and air-dried either under the fume hood for 1 hour or at benchtop overnight. Then they are stained with 0.4% SRB in 1% acetic acid, for 10 minutes in dark, and washed 3-5 times with 1% acetic acid to get rid of excess, unbound dye. After air drying, 10mM Tris base solution is added onto the wells to dissolve the protein-bound dye, from which an OD reading is obtained at the plate reader at 405nm.

4. RESULTS

4.1 FAM134B in Humans & Mouse

This section provides introductory gene and protein information on FAM134B in *Homo sapiens* and *Mus musculus*, obtained from the databases of the NCBI (National Center for Biotechnology Information) and Ensembl.

4.1.1 FAM134B Gene & Transcript Information

FAM134B is a protein-coding gene. The gene name FAM134B stands for "Family with sequence similarity 134, member B." Other aliases for the human gene include JK1, FLJ20152, FLJ22155, and FLJ22179, and its NCBI GeneID is 54463. The human FAM134B gene is located of chromosome 5, while mouse FAM134B gene is located on chromosome 15.

The human FAM134B gene encodes two transcripts produced by alternative splicing. Transcript variant 1 (NM_001034850, gi|77917616) has a linear full-length mRNA of 3259 bps (basepairs), and the translated region is 1494 bps. Transcript variant 2 (NM_019000, gi|77917615) has an mRNA length of 3108 bps, and the translated region is 998 bps. 6 exons at the 3' ends of the two transcripts are identical, and transcript 1 has 3 additional unique exons while transcript 2 has 1 additional unique exon at the 5' ends;

Figure 4.1: Genomic region and transcripts of FAM134B.

The mouse FAM134B gene, on the other hand, encodes 6 mRNA transcripts, also produced by alternative splicing of exons.

4.1.2 Protein Information on FAM134B

The two transcripts of human FAM134B code for two different FAM134B protein isoforms. Isoform 1 (NP_001030022) is 497 amino acids long, making up a protein of about 55kDa (kilo daltons) in mass, while isoform 2 (NP_061873) is 356 amino acids long, making up a protein of about 39 kDa. In western blots, both isoforms appear to have a higher mass than predicted, possibly due to post-translational modifications.

4.1.2.1 Domains, Motifs and Possible Sites of Post-Translational Modifications on the FAM134B Protein

Human FAM134B protein isoform 1 has two transmembrane domains at the N-terminal end, and one coiled coil domain at the C-terminal end, while isoform 2 has 1 transmembrane domain at the N-terminal end and one coiled-coil domain at the C-terminal end.

A review titled "Further assembly required: construction and dynamics of the endoplasmic reticulum network" published in EMBO Reports in 2010 draws attention to the fact that the FAM134 family proteins each have a pair of long hydrophobic segments similar to those found in reticulons and DP1/REEPs/Yop1, and that the members of the FAM134 family proteins may therefore be a new family of organelle-shaping proteins [35].

The SWISSPROT MotifScan tool also predicts that the FAM134B proteins may have sites for phosphorylation, N-glycosylation, and N-myristoylation. Possible phosphorylating candidates will be discussed later in detail.

4.1.3 Initial Findings on FAM134B

The FAM134B gene initially caught attention in our lab as a possible replicative senescence associated gene; increased FAM134B expression was detected in the replicative senescent Huh7 clones in comparison with the immortal counterparts [41]. Previous findings in our lab also suggested that the more poorly-differentiated

HCC cell lines had higher levels of FAM134B protein compared to the more well-differentiated HCC cell lines, and that this may be associated with the elevated ER stress levels of the poorly-differentiated cell lines [40].

4.2 FAM134B in Endoplasmic Reticulum Stress *in vivo*

Since previous findings by our group implicated that elevated levels of FAM134B protein may be associated with elevated levels of ER stress in HCC cell lines [40], we wished to further investigate this possibility *in vivo* as well.

4.2.1 Tunicamycin-induced ER stress causes a steatosis-like appearance in mice liver tissues

Tunicamycin is an antibiotic mixture that is commonly used for the induction of ER stress. Tunicamycin prevents the N-glycosylation of proteins in the ER, causing the accumulation of proteins in the ER, leading to ER stress.

Treatment of mice for 8 hours with 1ug/g body weight tunicamycin injected intraperitoneally lead to the appearance of a steatosis-like appearance in the liver tissues as seen in Figure 4.2. The liver tissues were stained with the Haematoxylene & Eosin staining technique which excludes lipids, causing the appearance of white, unstained regions. As seen in Figure 4.1, the tunicamycin treated mice liver tissues displayed lipid accumulation in the cytoplasms of the hepatocyte cells.

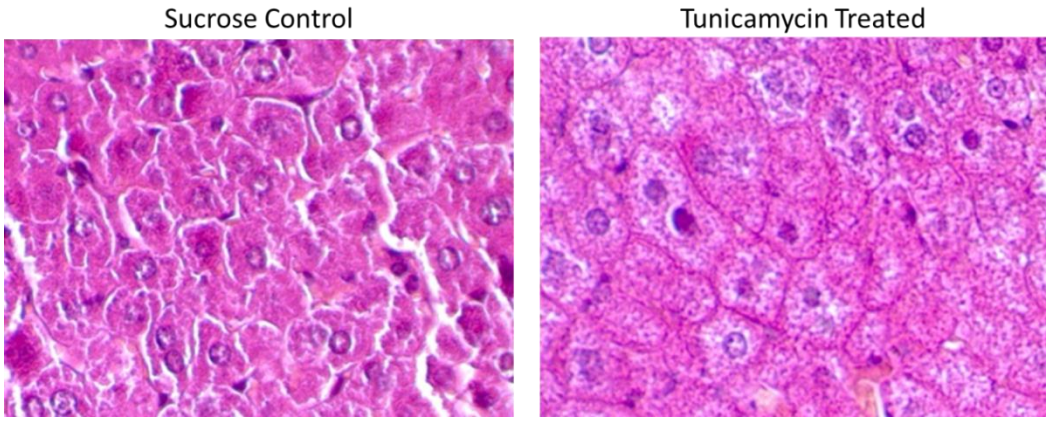

Figure 4.2: 8 hours of 1ug/g body weight tunicamycin treatment causes lipid accumulation and a steatosis-like morphology in mice liver tissue.

4.2.2 FAM134B expression is not affected in tunicamycin-induced ER stress in mice liver tissues

As seen in the Reverse-Transcription PCR results provided in Figure 4.3, 8 hours of induction of ER stress by tunicamycin treatment did not affect the mRNA expression levels of FAM134B, despite the visible splicing of XBP-1, which is an indicator of ER stress downstream of IRE1 in the unfolded protein response, as described previously.

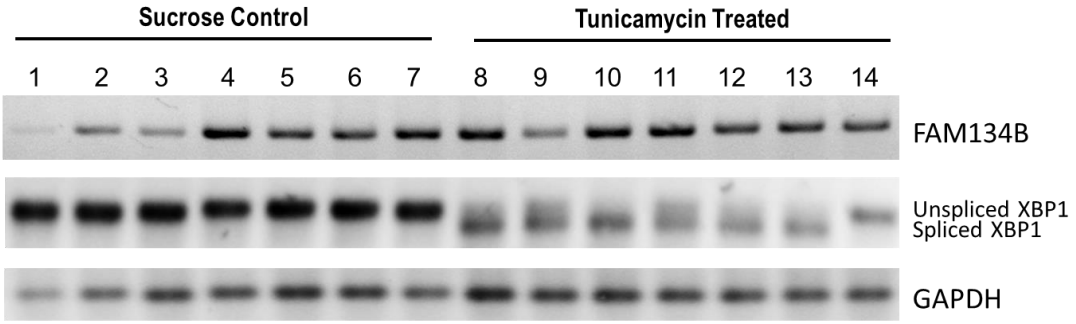

Figure 4.3: ER stress induction by 8 hours of 1ug/g body weight tunicamycin treatment does not affect the levels of FAM134B mRNA expression in liver tissues of mice. Each number represents a different mouse; 7 mice were injected with sucrose, and 7 with tunicamycin.

4.2.3 FAM134B protein level is not affected in tunicamycin-induced ER stress in mice liver tissues

As demonstrated in the western blotting results provided in Figure 4.4, tunicamycin treatment does not affect the protein levels of FAM134B in mice liver tissues, even though there is a significant elevation in the levels of phosophorylated eIF2α, which is an indicator of ER stress downstream of PERK in the unfolded protein response.

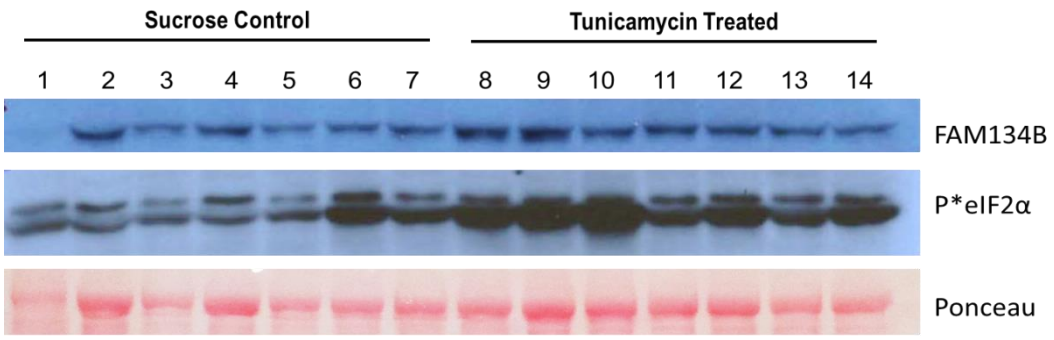

Figure 4.4: ER stress induction by 8 hours of 1ug/g body weight tunicamycin treatment does not affect the protein levels of FAM134B significantly in liver tissues of mice. Each number represents a different mouse; 7 mice were injected with sucrose, and 7 with tunicamycin.

4.3 FAM134B *in vitro*

4.3.1 Basal Levels of FAM134B in HCC cell lines

4.3.1.1 CCLE FAM134B Expression Data in HCC cell lines

The Cancer Cell Line Encyclopedia (CCLE) of the Broad Institute was utilized to select HCC cell lines with low and high expression levels of FAM134B. As seen in Figure 4.5, Hep3B, Huh7 and PLC cell lines have lower expression values, while Snu387, Snu398, Snu449 and Snu475 cell lines have higher expression values.

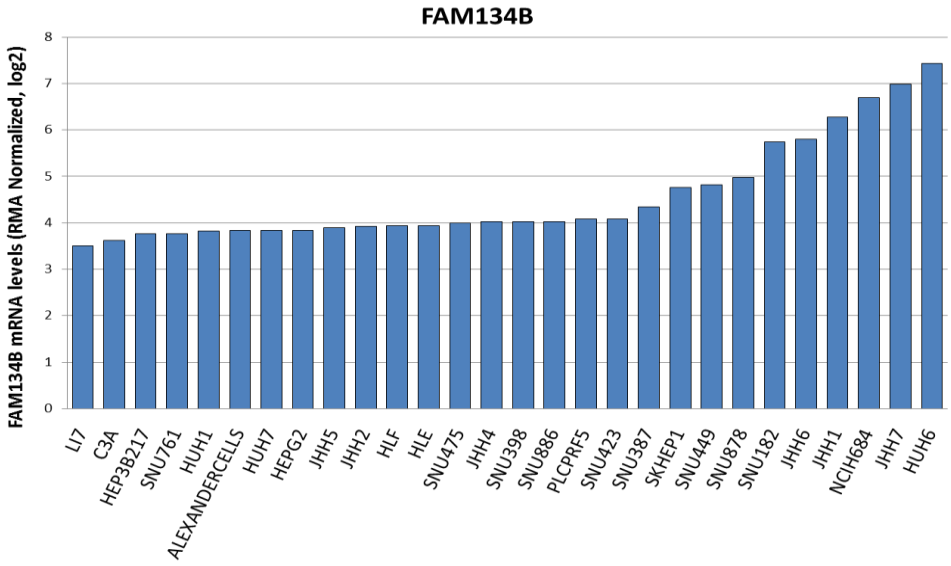

Figure 4.5: Relative FAM134B mRNA levels from the CCLE database.

4.3.1.2 Basal mRNA Expression levels of FAM134B in selected HCC cell lines

Semi-quantitative RT-PCR was performed on selected HCC cell lines to determine their FAM134B mRNA levels.

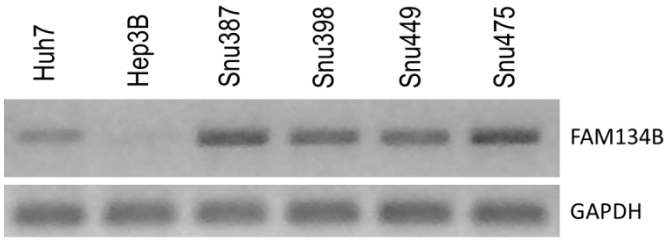

Figure 4.6: Basal FAM134B mRNA levels of selected HCC cell lines.

4.3.1.3 Basal Protein levels of FAM134B in selected HCC cell lines

Western blot was performed in order to determine the basal FAM134B protein levels in the selected cell lines. PLC, Huh7 and Hep3B cells, which are considered to be well-differentiated and more epithelial-like due to their cell morphology and vimentin expression levels [42], had very low FAM134B protein levels, while Snu387, Snu398, Snu475, and Snu449 cells, which are considered to be poorly-differentiated and more mesenchymal-like, had much higher levels of FAM134B protein levels.

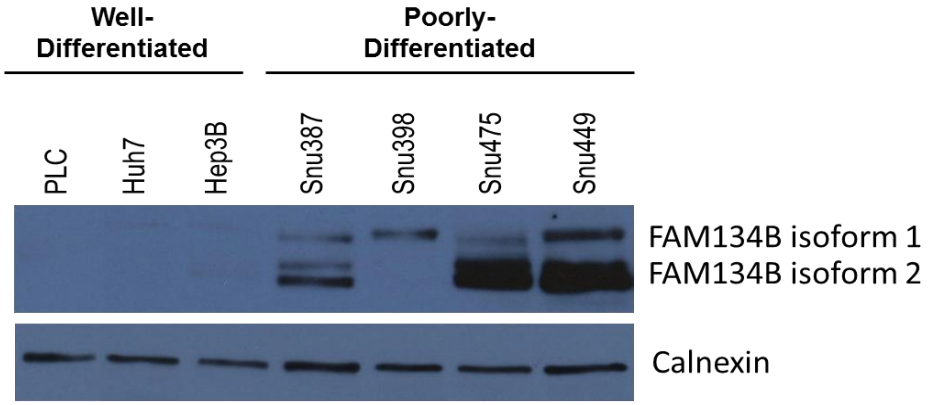

Figure 4.7: Basal FAM134B protein levels were higher in the more poorly-differentiated HCC cell lines compared to the well-differentiated HCC cell lines selected. The heavier band represents FAM134B isoform 1, while the lower band represents isoform 2.

Previous findings in our lab demonstrated that the overexpression of FAM134B does not induce Epithelial-to-Mesenchymal Transition (EMT) [40], therefore, it is likely that the elevated levels of FAM134B in the poorly differentiated cell lines is not a cause but a result of EMT, and this will be investigated further.

4.3.1.4 Sub-cellular localization of FAM134B protein in Snu387 cells

Immunoperoxidase staining of Snu387 cell lines was performed with the FAM134B antibody in order to observe the sub-cellular localization of the FAM134B protein. As can be observed in Figure 4.8, FAM134B demonstrates a perinuclear staining like that of Calnexin, which is indicative of localization on the Endoplasmic Reticulum.

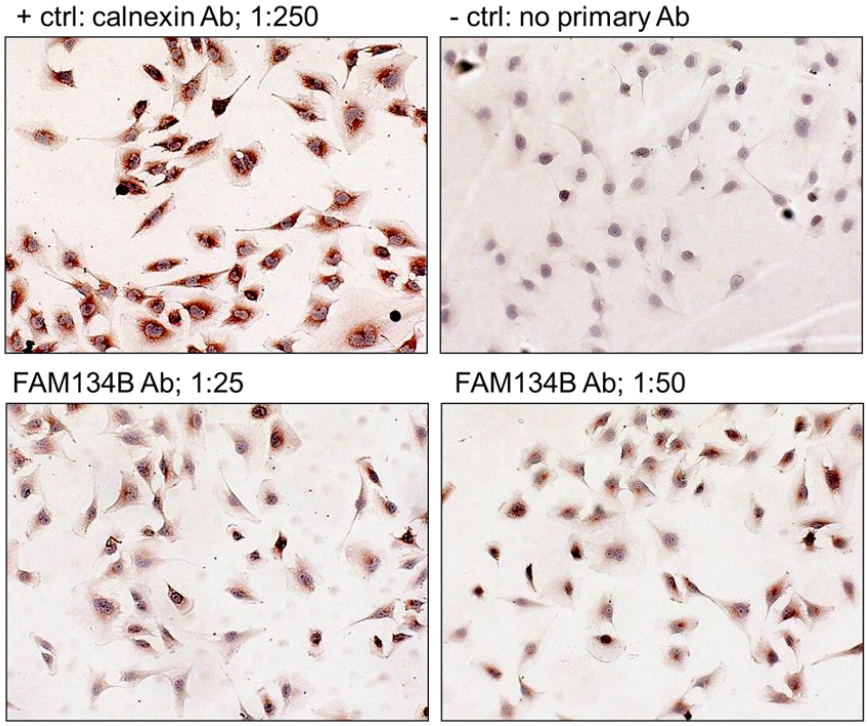

Figure 4.8: FAM134B demonstrates a perinuclear staining like that of Calnexin, which indicates localization on the Endoplasmic Reticulum.

4.3.2 FAM134B and ER stress

4.3.2.1 ER stress does not significantly affect mRNA expression levels of FAM134B in selected HCC cell lines

Tunicamycin, thapsigargin and dithiothreitol (DTT) are well-characterized ER stress inducers. Thapsigargin inhibits the sarco-endoplasmic reticulum Ca^{2+} ATPases (SERCA); this causes the ER to be unable to pump calcium from the cytosol to the ER lumen [43]. DTT breaks disulfide bonds, which causes proteins to unfold.

As seen in Figure 4.9, when ER stress was induced in Huh7, Snu387, Snu449 and Snu475 cell lines using these three ER stress inducers at different concentrations for 1, 6 and 24 hours, there was no significant effect on the mRNA levels of FAM134B, even when there was clear splicing of XBP-1, which marks ER stress.

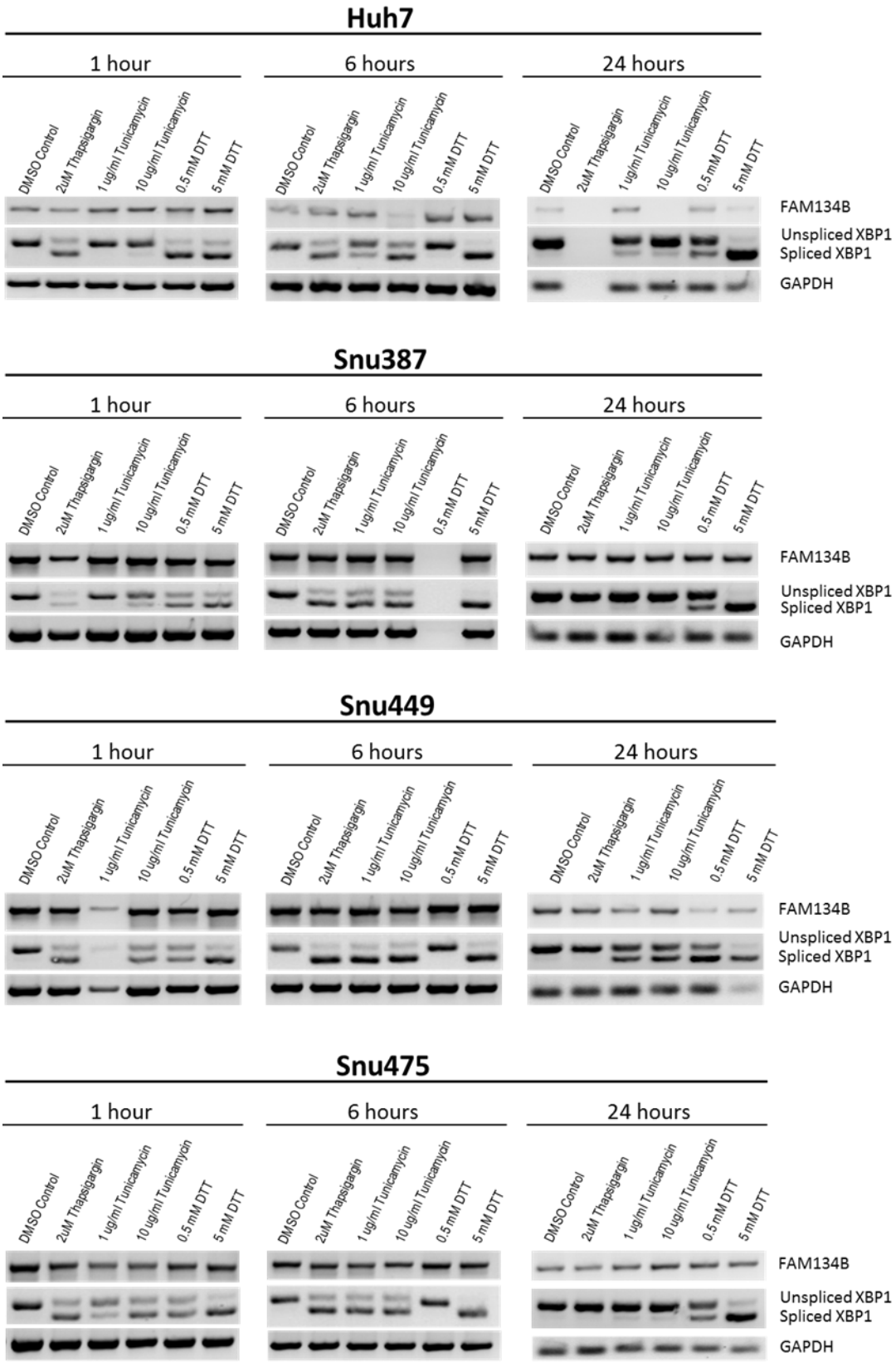

Figure 4.9: In Huh7, Snu387, Snu449 and Snu475 cell lines, FAM134B mRNA expression levels are not significantly affected by ER stress induction with Tunicamycin, Thapsigargin and DTT for 1, 6 and 24 hours.

4.3.3 Effect of 6 hours of ER stress induction on FAM134B protein levels in selected HCC cell lines

Western blotting was performed in order to detect changes in FAM134B protein levels in response to 6 hours of 2µM thapsigargin, 10µg/ml tunicamycin and 5mM DTT treatment, and there was no significant change at the protein level either.

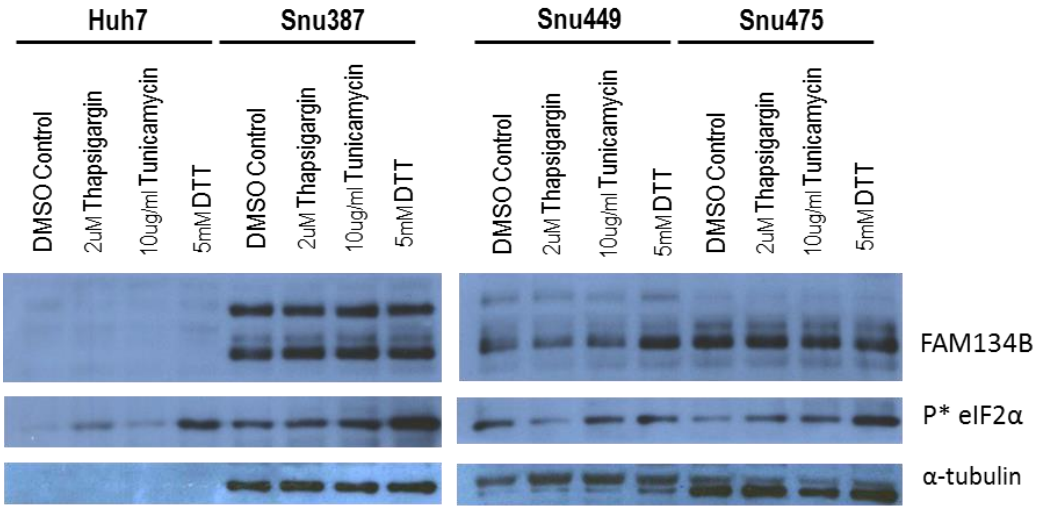

Figure 4.10: 6 hours of ER stress induction with tunicamycin, thapsigargin and DTT does not significantly affect FAM134B protein levels in selected cell lines, with the exception of DTT treatment in Snu449 cells.

The only exception was Snu449 cells, which demonstrated an increase in FAM134B protein in response to DTT treatment. Interestingly, as can be seen in Figure 4.11, Snu449 cells under DTT treatment were the only ones to demonstrate a significant ratio of cell death.

Figure 4.11 on the next page shows the cell morphologies and cell death patterns of the selected cell lines under 6 hours of different ER stress inducing treatments.

Also of note, in the western blot images in Figure 4.10 and Figure 4.7, there is a second, less abundant band right on top of the smaller isoform of the FAM134B protein. This may be indicative of a post-translational modification that has made a sub-group of FAM134B isoform 2 proteins slightly heavier than the rest, causing this band that is shifted.

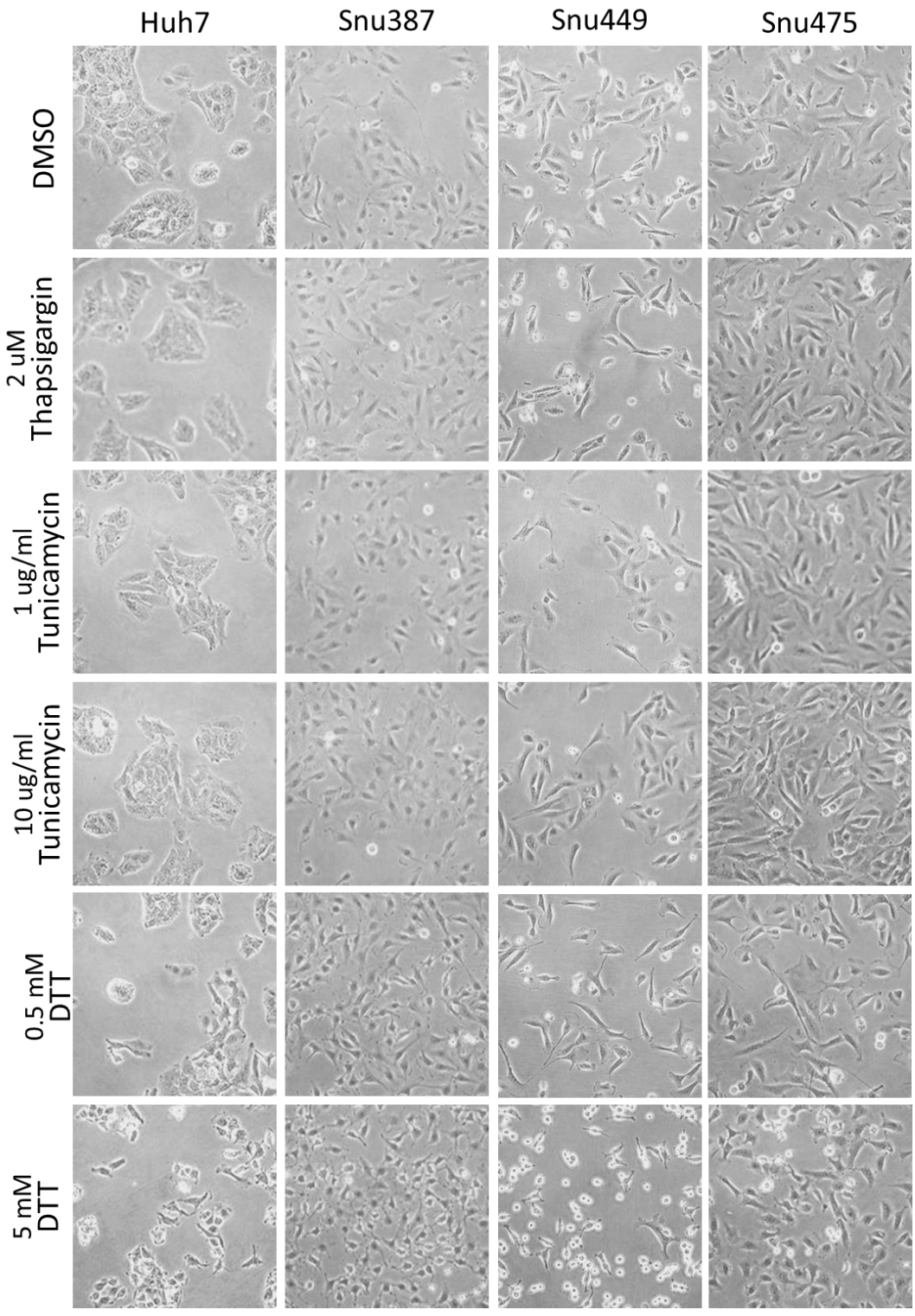

Figure 4.11: Cell morphology and cell death patterns under ER stress induction for 6 hours with different inducers. Snu449 cells under 5mM of DTT treatment for 6 hours showed a significant ratio of cell death.

4.3.4 FAM134B and EMT

4.3.4.1 Huh7, PLC and Hep40 cells display a more dispersed growth pattern upon 72 hours of TGF-β1 treatment

TGF-β induces Epithelial-to-Mesenchymal Transition (EMT) by triggering the activation of the transcription factors Snail, ZEB and Twist, which regulate the upregulation of mesenchymal markers such as Vimentin and downregulation of epithelial markers such as E-cadherin [44].

In order to induce EMT in the more well-differentiated HCC cell lines Huh7, PLC and Hep40, cells were treated with 2ng/ml and 4ng/ml TGF-β1 for 72 hours. As seen in Figure 4.12, the cells displayed a more dispersed morphology after this treatment.

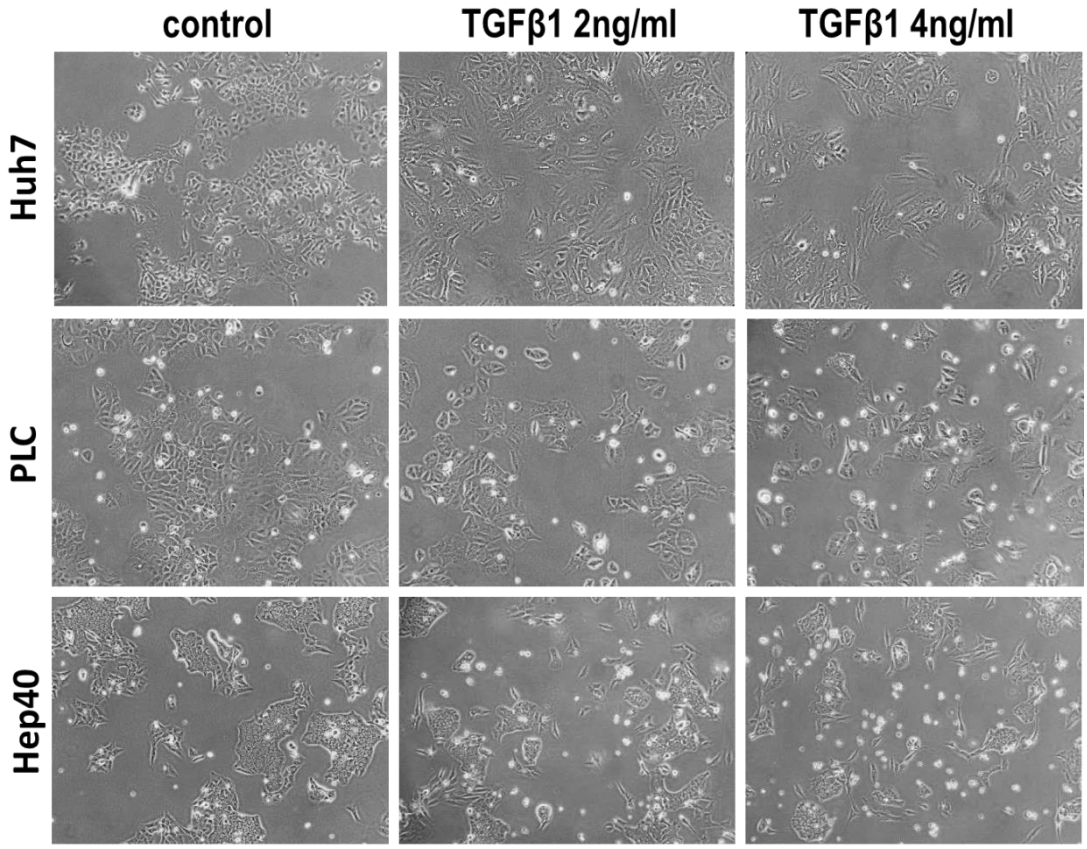

Figure 4.12: The well-differentiated HCC cell lines Huh7, PLC and Hep40 assume a more mesenchymal-like morphology after 72 hours of treatment with TGF-β1.

4.3.4.2 Upon EMT induction, PLC cells display a dramatic increase in Vimentin, accompanied by an increase in FAM134B protein levels

PLC cells were the cell line that exhibited the most apparent morphological changes upon induction of EMT with 72 hours of TGF-β1 treatment. As demonstrated by the western blot and the graphs in Figure 4.13, the Vimentin levels of PLC cells increased dramatically, and this increase in Vimentin levels was accompanied by an elevation in FAM134B levels.

Proteins such as actin, calnexin or tubulin which are normally used as loading controls could be affected by EMT induction by TGF-β1, therefore the Ponceau staining was taken into consideration when making sure of equal loading.

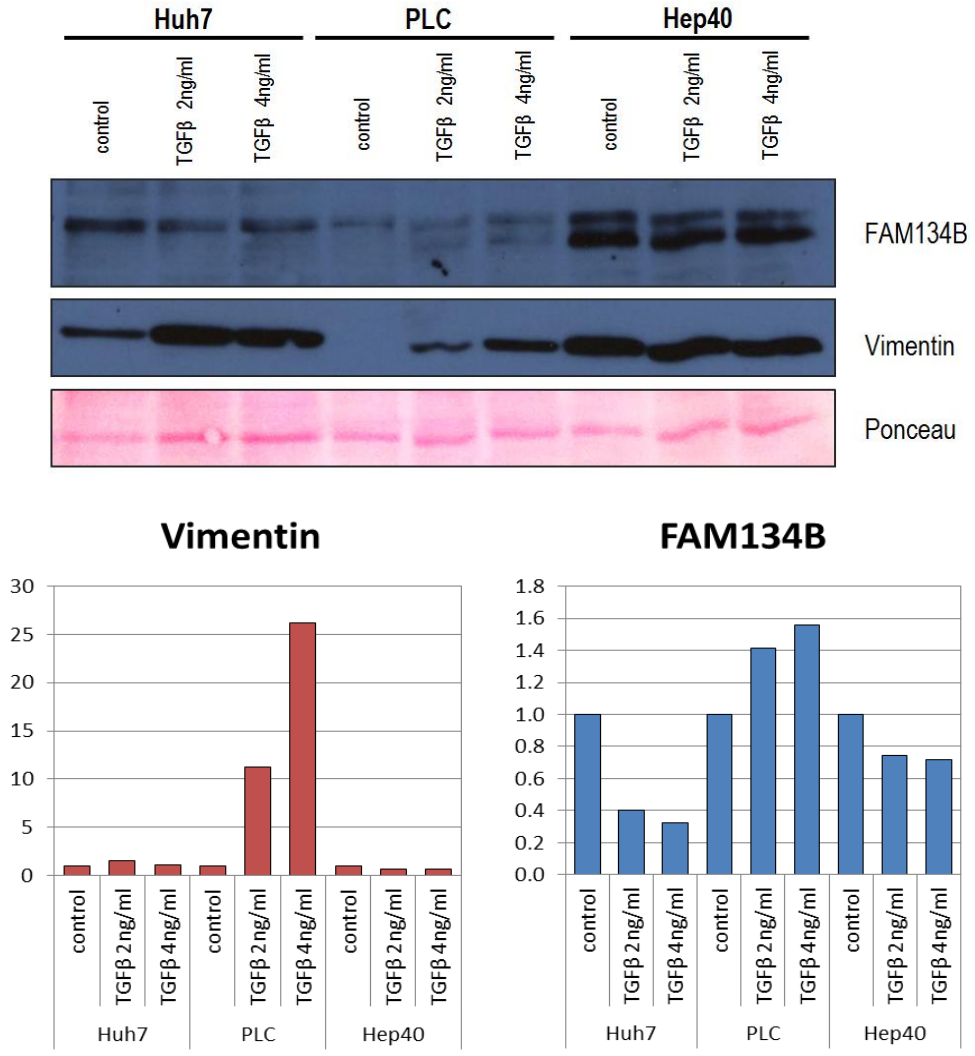

Figure 4.13: Western blot and graph of relative expression levels normalized to the Ponceau staining demonstrate a dramatic increase in Vimentin levels in PLC cells, which is accompanied by an increase in FAM134B levels.

4.3.5 FAM134B knockdown experiments in Snu449 cells

4.3.5.1 Successful silencing of FAM134B with shRNA transfection

Stable transfection of Snu449 cells with shRNA constructs against FAM134B mRNA was performed by previous group members (P. Telkoparan, H. Alotaibi, N. Taşdemir, of M. Öztürk Lab). Cells were maintained with puromycin in culture to ensure persistence of knockdown cells, and western blots were performed to assess protein levels of FAM134B in the knockdowns. As seen in Figure 4.14, FAM134B protein levels were reduced to about 40% in two clones, 59-11 and 59-12, while the scrambled control RNA appeared to cause overexpression of FAM134B protein.

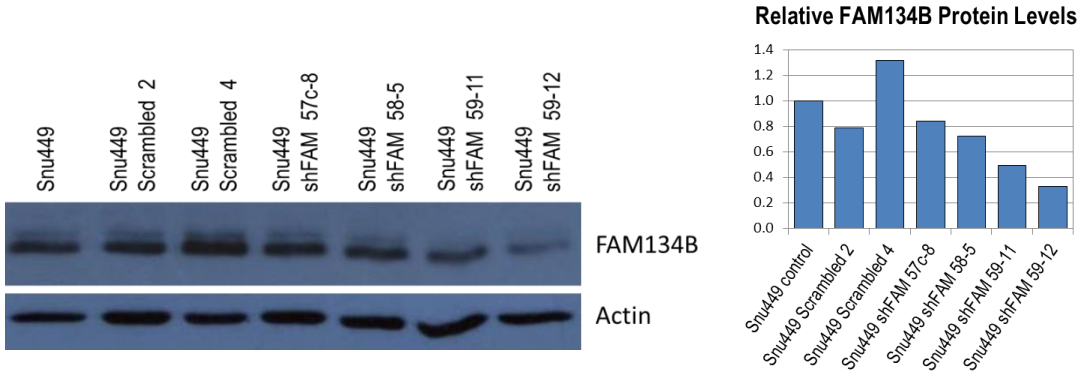

Figure 4.14 : shRNA knockdown of FAM134B is effective, especially in clones 59-11 and -12.

These results were confirmed also at the mRNA level with semi-quantitative Reverse Transcription PCR using the selected clones, as can be seen in Figure 4.15.

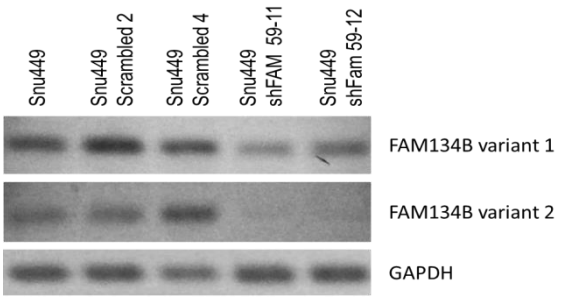

Figure 4.15: shRNA silencing of FAM134B is also visible at the mRNA level in clones 59-11 and -12.

4.3.5.2 FAM134B-silenced Snu449 cells display an altered morphology in culture

As seen in Figure 4.16, the Snu449 shFAM134B 59-11 and 59-12 clones displayed a more elongated morphology in cell culture that is typical of the more mesenchymal-like, poorly differentiated HCC cell lines, compared to the more round and grouped morphology of the more epithelial-like cell lines.

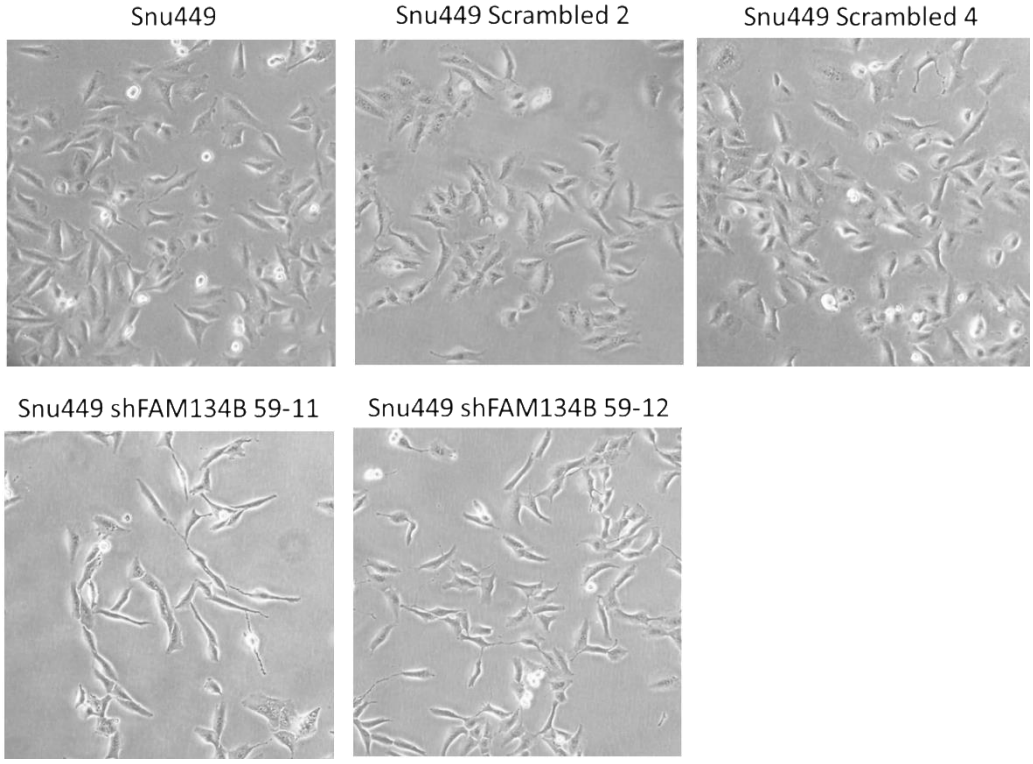

Figure 4.16: FAM134B-silenced Snu449 cells displayed an altered morphology in culture.

4.3.5.3 Despite having an elongated, more mesenchymal-like appearance in culture, FAM134B knockdown Snu449 cells did not have an increase in Vimentin levels or migration capacity

We had previously suspected that the elevated levels of FAM134B protein in the more mesenchymal-like cell lines may be a consequence of EMT, and in PLC cell lines, induction of EMT and increase in Vimentin appeared to cause some increase in FAM134B levels. Therefore, it was surprising to observe a more elongated, mesenchymal-like appearance in the FAM13B knockdown Snu449 cells. We

investigated further by assessing the Vimentin expression levels, but there was no significant increase, as seen in Figure 4.17.

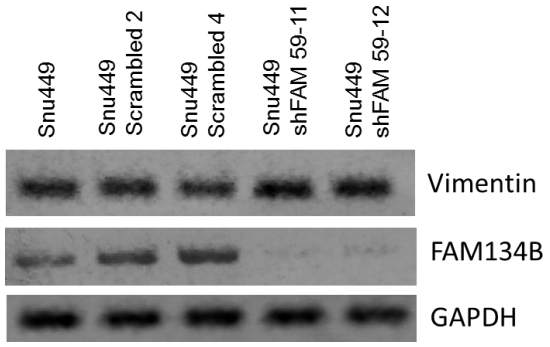

Figure 4.17: Vimentin levels are not significantly increased in FAM134B knocked-down Snu449 cells.

We also wished to asses any changes in the migratory capacity of the FAM134B-silenced Snu449 cells with a wound-healing assay. Interestingly, as seen in Figure 4.18, the FAM134B-silenced Snu449 cells had a slightly reduced migratory capacity.

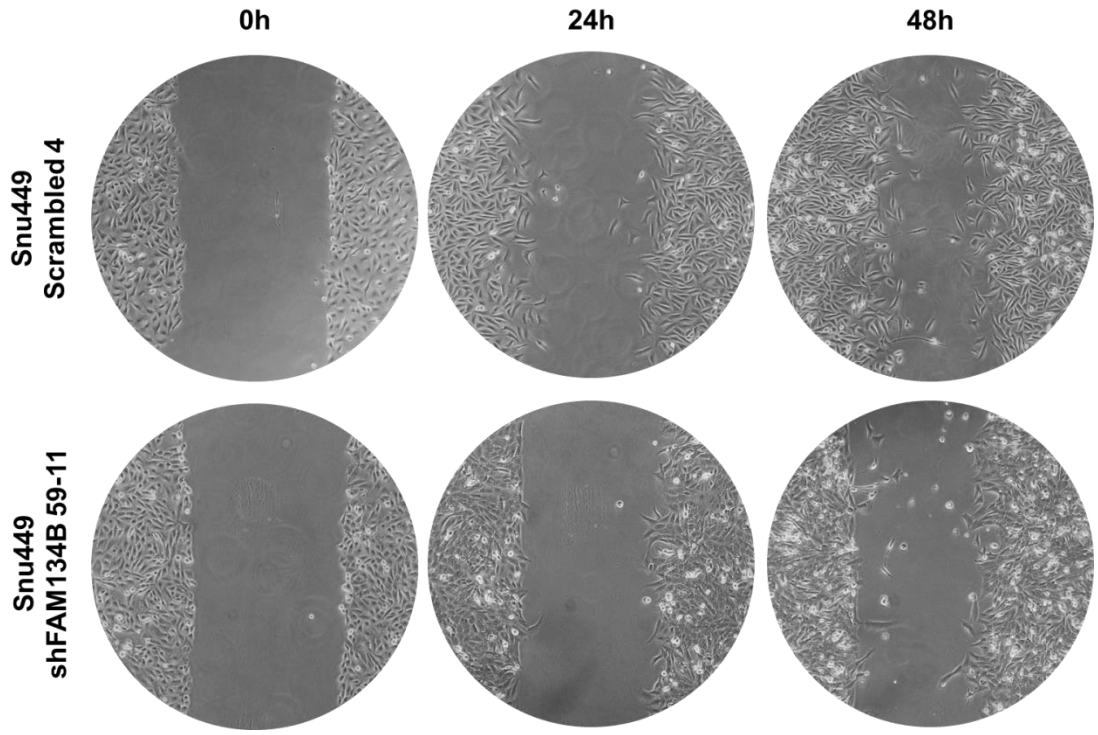

Figure 4.18: FAM134B-silenced Snu449 cells had poorer survival and migratory capabilities under serum starved conditions that inhibited proliferation.

In the scratch assay shown in Figure 4.18, 24 hours after the cells were plated, the medium of the cells were switched from 10% serum to 0.05% serum in order to prevent proliferation of the cells so that cell movement could be detected accurately. It caught our attention that there was more cell death in the FAM134B-silenced Snu449 cells under serum starvation conditions, which was validated with an SRB experiment as follows.

4.3.5.4 FAM134B-silenced Snu449 cells have poorer survival capabilities under serum starvation conditions

The sulforhodamine B (SRB) colorimetric assay was used to establish survival rates of FAM134B-silenced Snu449 cells versus control cells under cytotoxic conditions. SRB is a red, water-soluble, fluorescent dye that is used for the quantification of cellular proteins of cultured cells as a means of determining cell density [45].

In the graph in Figure 4.19, the survival ratio of each cell type was determined by considering the cell density at 10% serum as the 100% survival mark of that particular cell type. As can be seen in the graph, FAM134B-silenced Snu449 cells have poorer survival capabilities under serum starvation conditions.

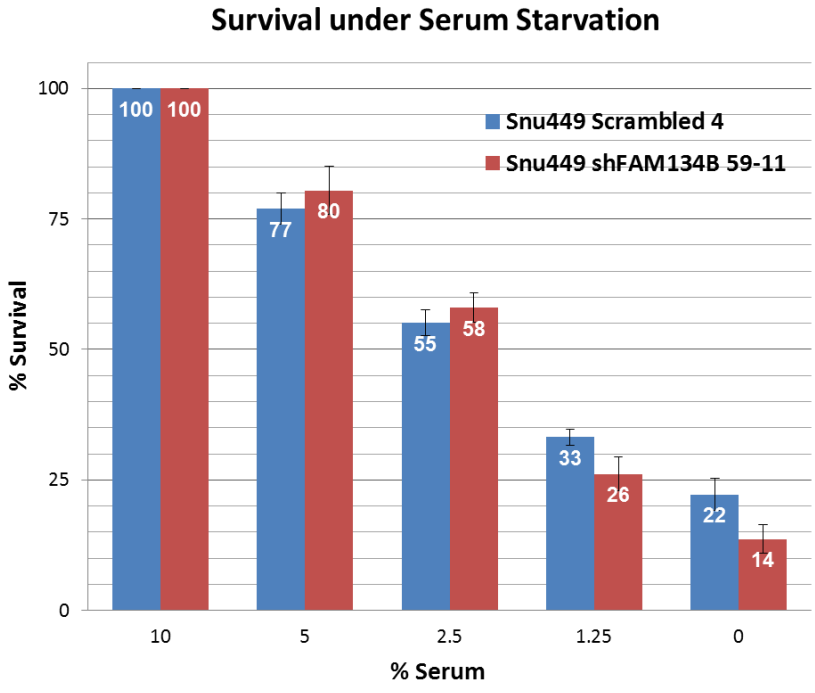

Figure 4.19: FAM134B-silenced Snu449 cells have poorer survival capabilities under serum starvation conditions.

4.3.6 Effects of FAM134B Knockdown on Cytotoxicity of Different Drugs

In this section, the SRB colorimetric assay was utilized in order to determine survival rates of different cell types after 72 hours of treatment with different cytotoxic drugs and conditions, and half maximal inhibitory concentration (IC50) values were determined for each treatment for each cell type. The assays were performed in 96-well plates in triplicates.

4.3.6.1 Snu449 cells have a very high resistance to thapsigargin

As previously cited, thapsigargin is an inhibitor of the sarco-endoplasmic reticulum Ca^{2+} ATPase (SERCA) pumps (encoded by the ATP2A3 gene) found on the endoplasmic reticulum membrane. Thapsigargin prevents the uptake of cytosolic calcium by the ER, causing depletion of calcium in the ER lumen and increase of calcium in the cytosol [43].

Analysis of the cytotoxicity of thapsigargin on the selected HCC cell lines revealed that Snu449 cells had the highest resistance to apoptosis induced by thapsigargin, as seen in Figure 4.20.

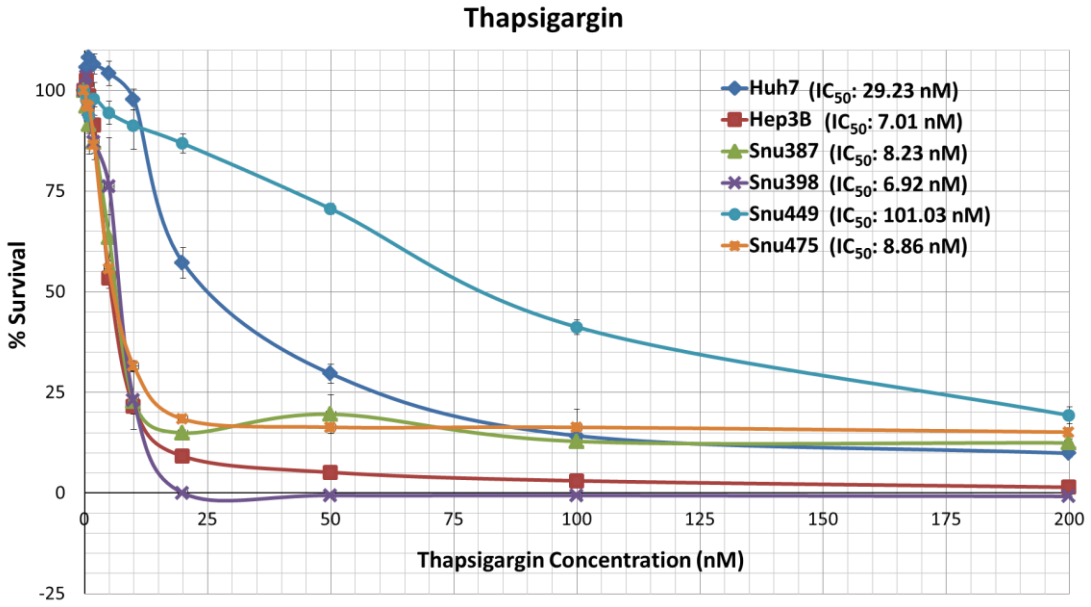

Figure 4.20: Snu449 cells have a significantly high resistance to thapsigargin.

4.3.6.2 Knockdown of FAM134B caused a dramatic loss of Thapsigargin resistance in Snu449 cells, indicating a calcium-associated function for the FAM134B protein

The effect of FAM134B silencing on the thapsigargin resistance capability of Snu449 cells was very dramatic; while the half maximal inhibitory concentration (IC50) was about 92.61nM for Snu449 Scrambled 4 control cells, the half maximal inhibitory concentration of thapsigargin was as little as 5.33nM in Snu449 shFAM134B 59-11 cells, as seen in Figure 4.21.

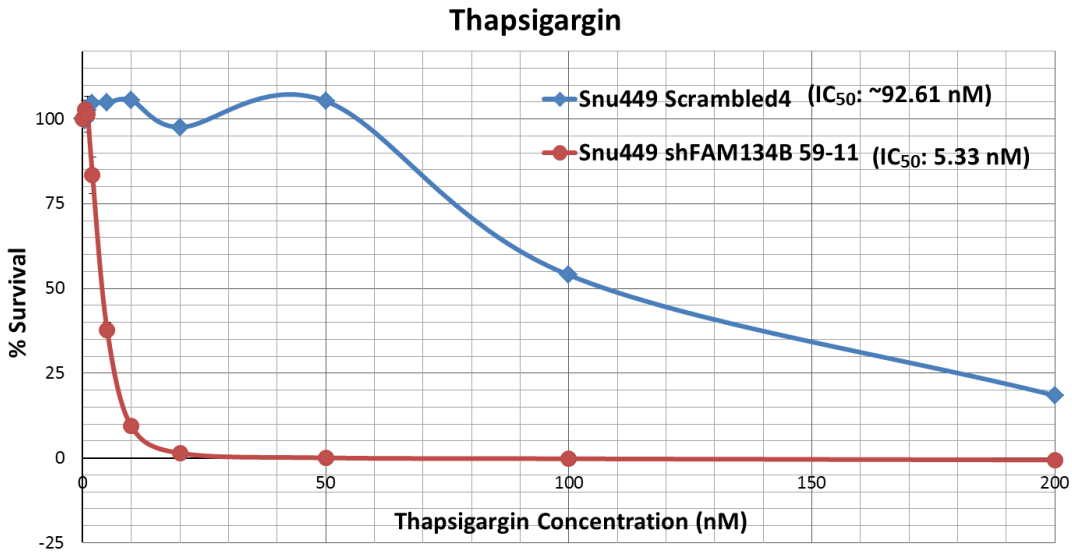

Figure 4.21: Silencing of FAM134B causes a dramatic decrease in thapsigargin resistance of Snu449 cells.

This dramatic loss of thapsigargin resistance upon silencing of FAM134B indicated that the FAM134B protein may have a role that is associated with calcium levels in the cell; FAM134B may either interact with the calcium pumps on the ER membrane to prevent the channel's inhibition by thapsigargin, or it may play a role in adapting cellular functions to conditions of high cytosolic calcium and low ER calcium.

Further experimenting with the cytotoxicity of different drugs to FAM134B-silenced Snu449 cells provided additional support for a specific, calcium-related function for FAM134B.

4.3.6.3 Knockdown of FAM134B also caused a dramatic loss of Adriamycin resistance in Snu449 cells

Adriamycin, or Doxorubicin, is a DNA intercalating agent that induces apoptosis primarily by causing DNA damage, but interestingly, it was also demonstrated to interfere with the sarco-endoplasmic calcium pumps of the cell, which was best studied in cardiac muscle cells, for which calcium signaling has vital roles [46].

Remarkably, FAM134B knocked-down Snu449 cells also demonstrated a very significant loss of Adriamycin resistance, as shown in Figure 4.22.

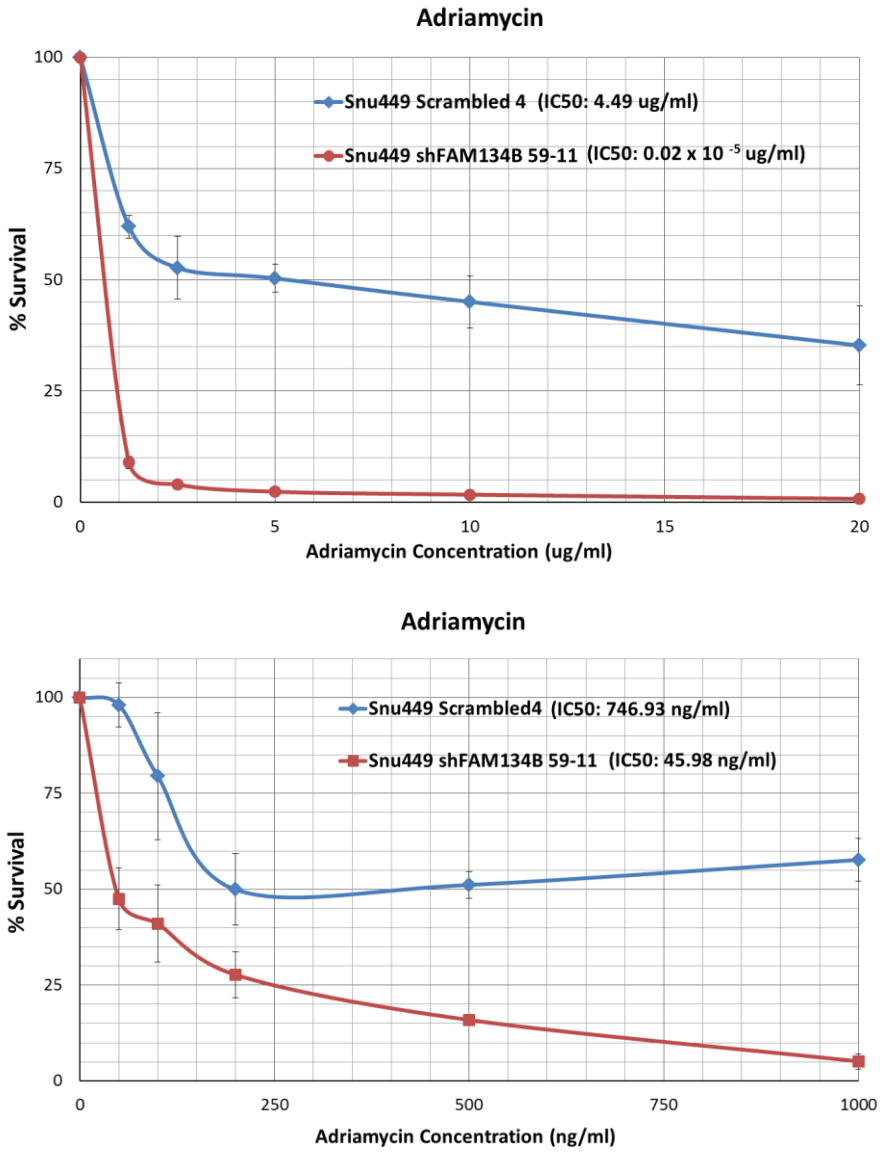

Figure 4.22: Silencing of FAM134B drastically reduces Adriamycin resistance in Snu449 cells both in higher ug/ml (top) and lower ng/ml (bottom) concentrations.

4.3.6.4 Tunicamycin resistance is not significantly affected by the silencing of FAM134B

Tunicamycin is an antibiotic mixture that causes ER stress through preventing N-glycosylation of nascent peptides in the ER.

SRB assays on the shRNA FAM134B knock-down Snu449 cells showed no effect of loss of FAM134B expression on the cytotoxicity of tunicamycin to Snu449 cells, as shown in Figure 4.23.

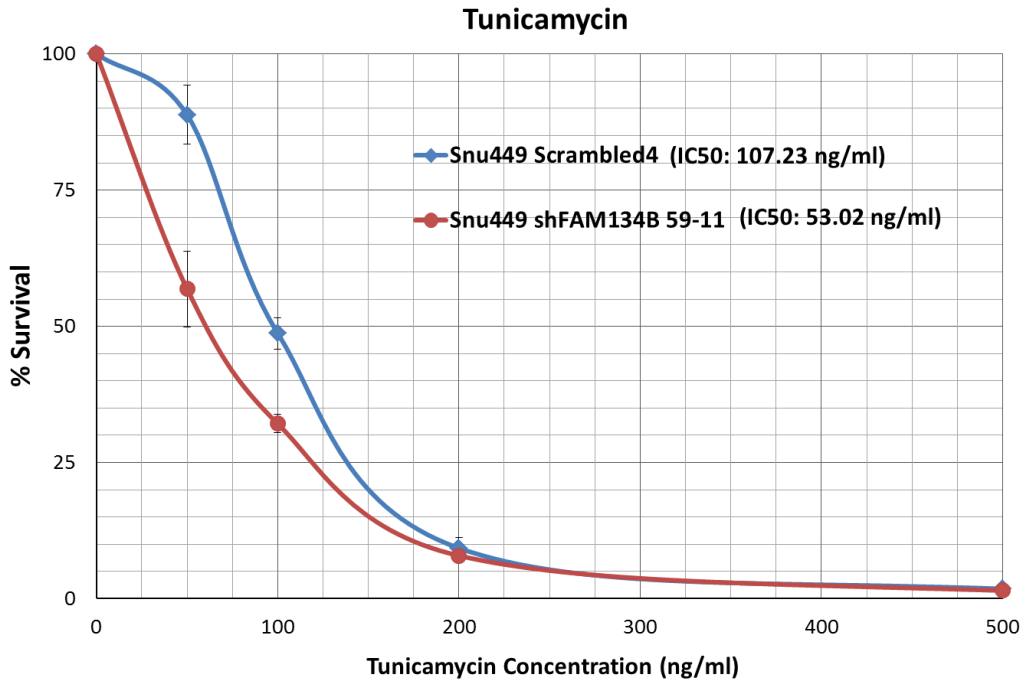

Figure 4.23: Tunicamycin cytotoxicity is not affected by the silencing of FAM134B.

This result draws further attention to the likelihood of a specifically calcium-related function for the FAM134B protein, because tunicamycin is also a very potent ER stress inducer like thapsigargin, however, the cytotoxicity of tunicamycin does not seem to be affected by loss of FAM134B expression. Therefore, FAM134B is likely to have a role that is specifically related to the calcium pumps on the ER membrane rather than ER stress in general, since resistance to thapsigargin and Adriamycin are both severely altered, and these two drugs are known to inhibit the ER calcium pump.

4.3.6.5 FAM134B silencing enhances antitumor activity of TGF-β

TGF-β causes G1 arrest and senescence in HCC cell lines, leading to an antitumor activity, as demonstrated previously by our group [47]. Figure 4.24 shows that FAM134B-knocked-down Snu449 cells had reduced survival rates. Intriguingly, TGF-β was also shown to increase intracellular levels of Ca^{2+}, as well as inositol triphosphate (IP_3) which plays key roles in calcium homeostasis [48]

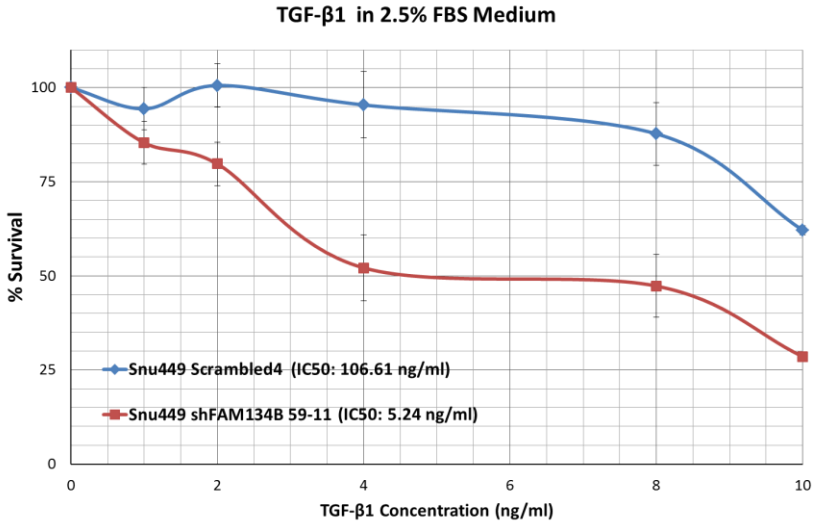

Figure 4.24: FAM134B silencing enhances antitumor activity of TGF-β.

4.3.6.6 FAM134B silencing only slightly enhances EtOH-induced cell death

In order to detoxify ethanol, hepatocytes can double the surface area of their smooth ER for a few days [49]. Here, it was investigated whether FAM134B was essential in this process of overcoming an EtOH challenge, and there seemed to be some effect.

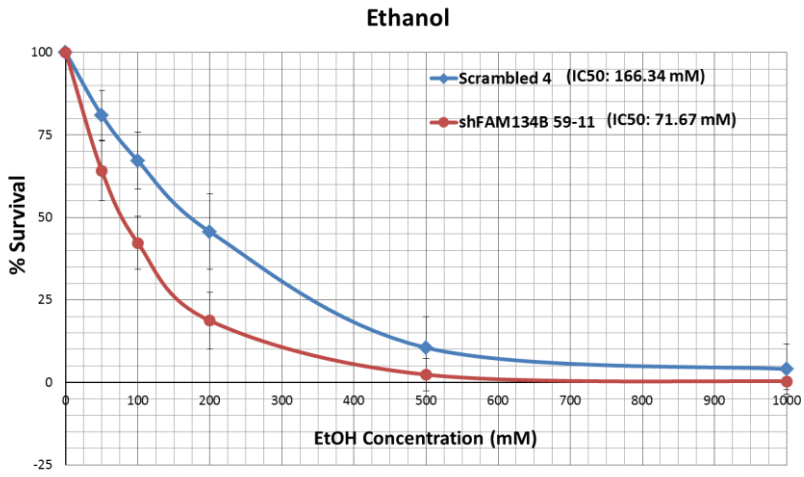

Figure 4.25: FAM134B silencing only slightly enhances EtOH-induced cell death.

4.3.6.7 Knockdown of FAM134B does not affect resistance of Snu449 cells to the anti-cancer drugs 5-fluorouracil and camptothecin

5-Fluorouracil (5-FU) is a drug pyrimidine analog that inhibits thymidylate synthase, leading to DNA damage [50]. Camptothecin binds and stabilizes the topoisomerase I and DNA complex that forms during DNA replication and transcription, causing DNA damage and apoptosis [51]. SRB assays did not reveal a significant difference between the survival rates of FAM134B-silenced Snu449 cells compared to scrambled control, as seen in Figure 4.26.

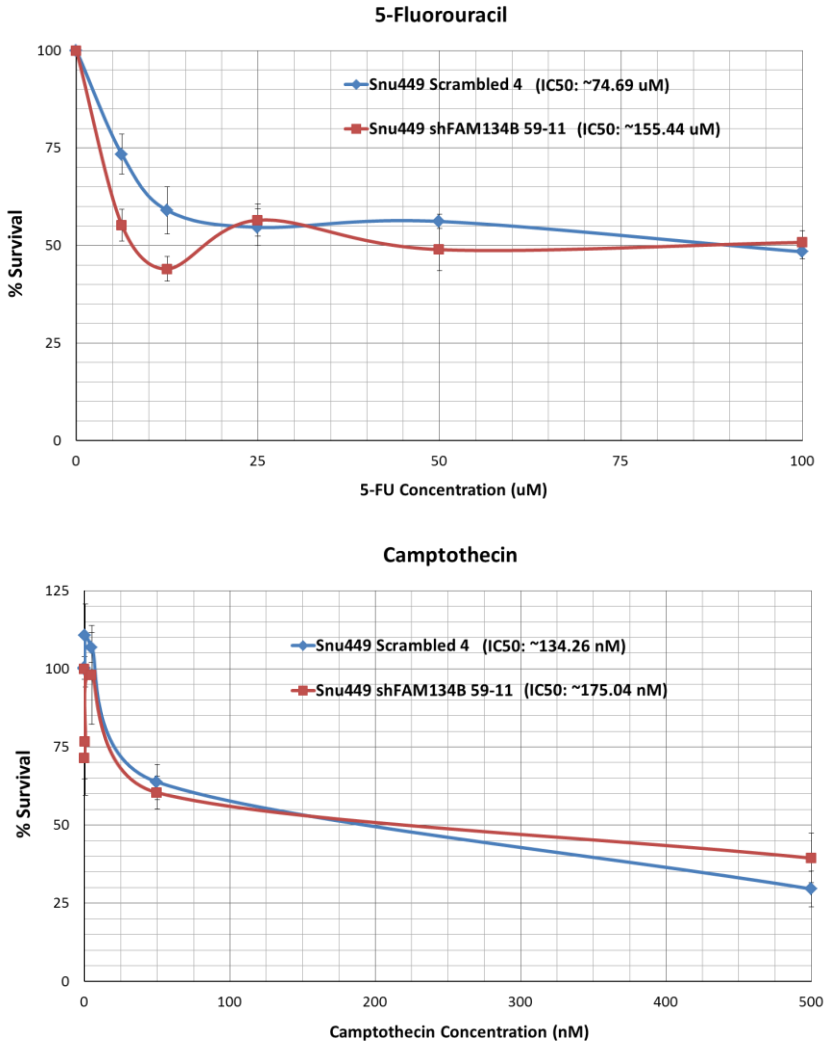

Figure 4.26: FAM134B silencing does not affect resistance to 5-fluorouracil and camptothecin induced cytotoxicity.

4.3.6.8 Knockdown of FAM134B does not significantly affect survival rates under oxidative stress induced by hydrogen peroxide

Hydrogen peroxide (H_2O_2) treatment gives rise to the free radical OH, which is a Reactive Oxygen Species (ROS) known to cause oxidative stress, lipid peroxidation, ER stress, and ultimately, apoptosis in cancer cells [52]. Therefore, possible differential survival rates under H_2O_2 treatment were also investigated to observe any difference in the FAM134B silenced cells in coping with oxidative stress. As seen in Figure 4.27, there was no significant difference in the survival rates of FAM134B knocked-down Snu449 shFAM134B 59-11 cells and Snu449 Scrambled 4 control.

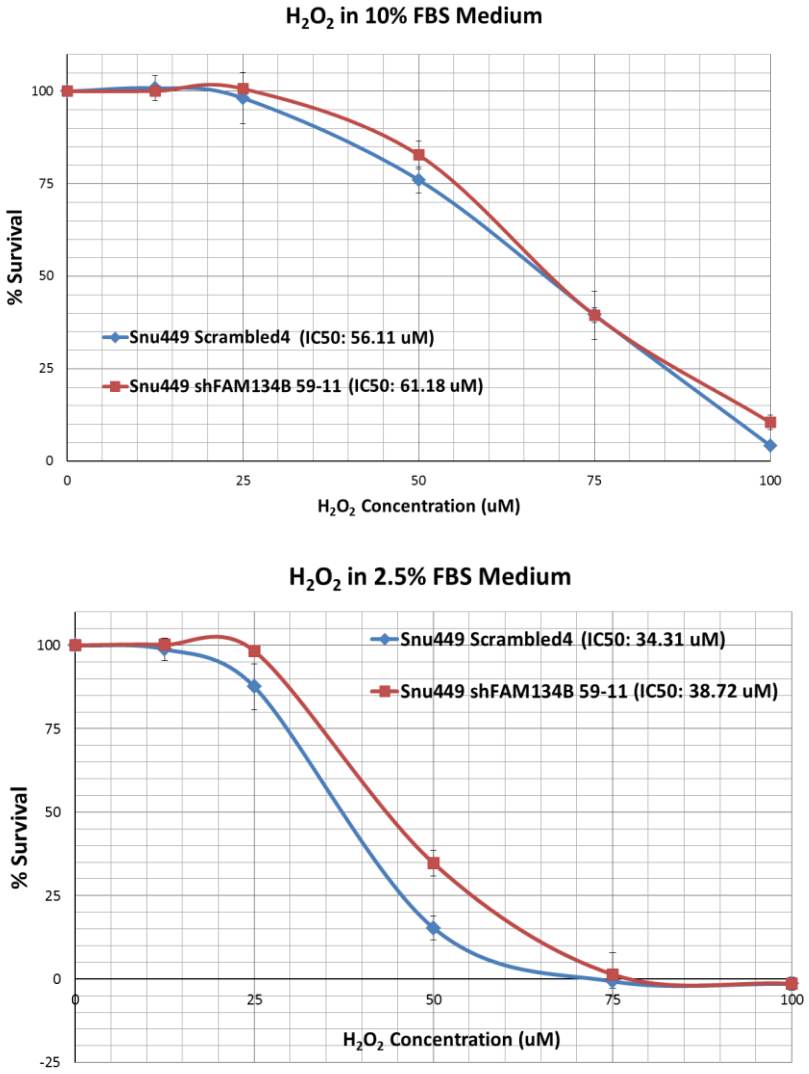

Figure 4.27: Silencing of FAM134B does not significantly affect survival rates under oxidative stress induced by H_2O_2.

4.4 Proteins predicted to phosphorylate FAM134B isoforms

Our western blot results indicated that the FAM134B protein may be subjected to post-translational modifications such as phosphorylation. And our SRB results demonstrated that FAM134B protein may be important in cell survival under several forms of cytotoxic drugs, such as tunicamycin. Further experimental work will need to performed in order to understand the function of the FAM134B protein, but here, an online predictive tool was utilized.

The Motif Scan tool found on the Scansite website (scansite.mit.edu) developed by Massachusetts Institute of Technology [53] was utilized in order to predict protein candidates that may be phosphorylating the two isoforms of the human FAM134B

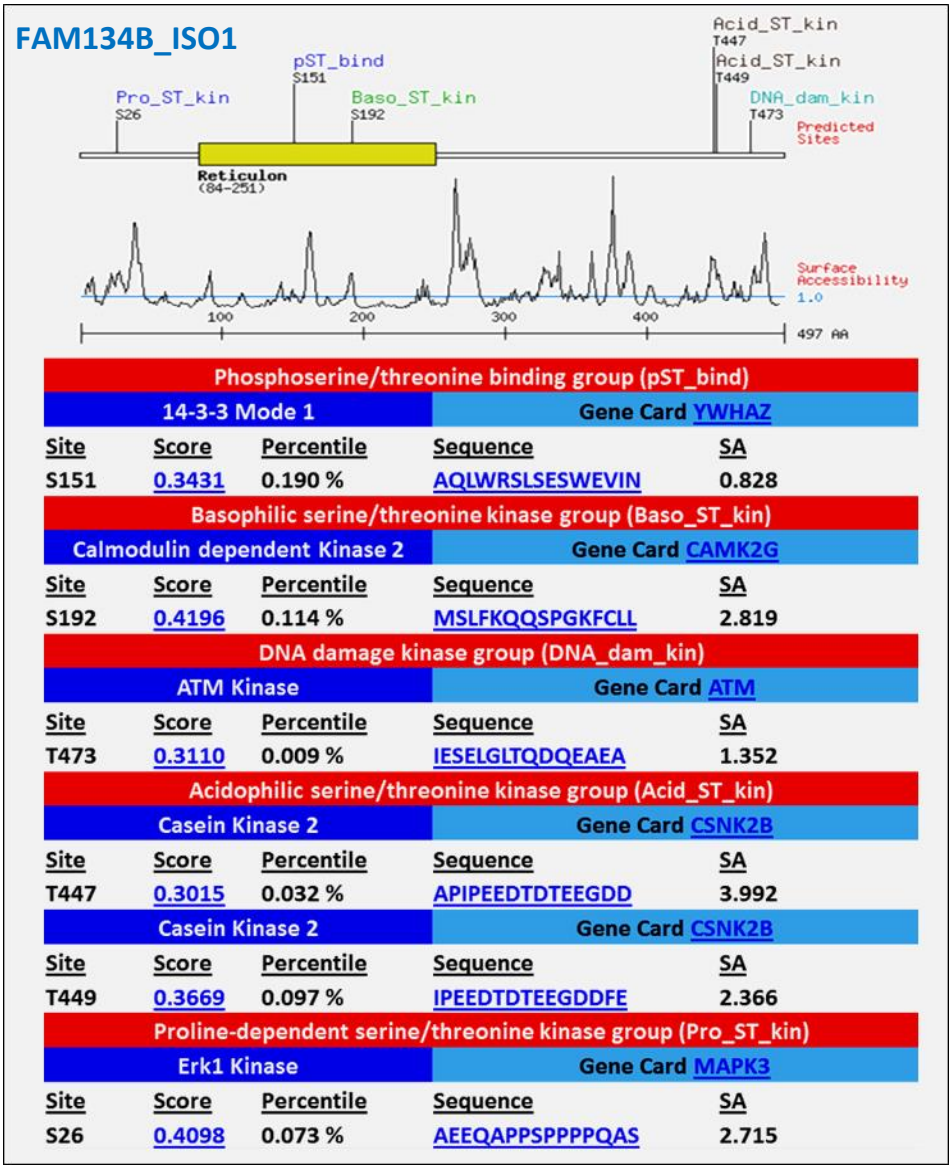

Figure 4.28: Protein candidates that are predicted to phosphorylate FAM134B isoform 1.

protein. This tool contains a database of the short consensus target sequences of several well-known kinases, and identifies these short regions on a protein sequence query.

Intriguingly, as seen in Figure 4.28, ERK1 kinase, ATM kinase, Calmodulin dependent kinase 2, Casein kinase and 14-3-3 mode 1 are among the proteins predicted to phosphorylate FAM134B isoform1, with very high stringency scores. A percentile score less than 0.2 is considered to have a high stringency, and several research papers have utilized the Scansite tool as a starting point and have managed to validate these predictions experimentally [54].

ERK1 kinase is particularly very interesting as a possible kinase that may be phosphorylating FAM134B. SRB assays using the FAM134B knockdown cells have demonstrated that the FAM134B protein is likely to have a function that is essential for cell survival under ER stress, especially when calcium channels are inhibited.

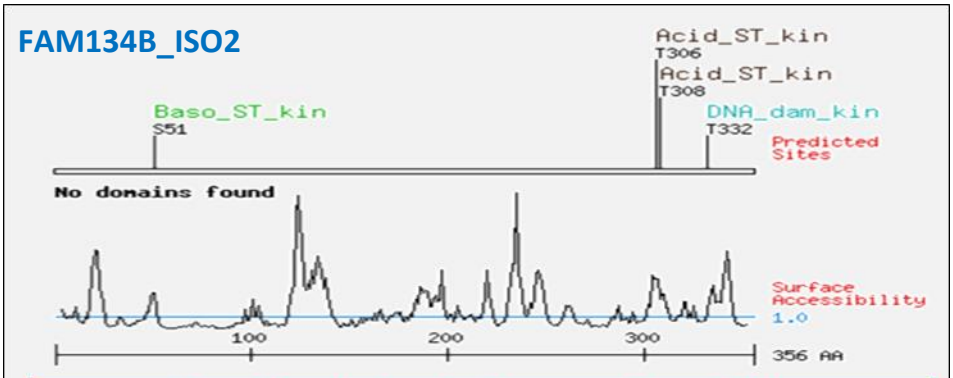

Basophilic serine/threonine kinase group (Baso_ST_kin)				
Calmodulin dependent Kinase 2			Gene Card CAMK2G	
Site	Score	Percentile	Sequence	SA
S51	0.4196	0.114 %	MSLFKQQSPGKFCLL	2.819
DNA damage kinase group (DNA_dam_kin)				
ATM Kinase			Gene Card ATM	
Site	Score	Percentile	Sequence	SA
T332	0.3110	0.009 %	IESELGLTQDQEAEA	1.352
Acidophilic serine/threonine kinase group (Acid_ST_kin)				
Casein Kinase 2			Gene Card CSNK2B	
Site	Score	Percentile	Sequence	SA
T306	0.3015	0.032 %	APIPEEDTDTEEGDD	3.992
Casein Kinase 2			Gene Card CSNK2B	
Site	Score	Percentile	Sequence	SA
T308	0.3669	0.097 %	IPEEDTDTEEGDDFE	2.366

Figure 4.29: Protein candidates that are predicted to phosphorylate FAM134B isoform 2.

Snu449 cells are known to have a high endogenous c-Src activity, promoting carcinogenesis through the Src/PI3K/Akt pathway [33] [34]. It is also known that the PI3K/Akt and MEK1/ERK pathways cross-talk and regulate survival under ER stress [25]. Therefore, it would be very interesting to experimentally determine whether FAM134B isoform 1 is indeed phosphorylated by ERK1 kinase.

Figure 4.29 demonstrates that, ATM kinase, Calmodulin dependent kinase 2 and Casein kinase 2 may also be among the kinases that may phosphorylate FAM134B isoform 2.

The other predicted candidates are also very interesting. Calmodulin dependent kinase 2 is a kinase that is essential for Ca^{2+} homeostasis as Calmodulin is a calcium modulated protein that transduces Ca^{2+} signals in the cell. 14-3-3 mode 1 is involved in the regulation of Akt, Raf1, Bad, Bax and Cdc25. ATM kinase targets p53, CHK2 and H2AX, aiding in DNA damage response, and is involved in cell cycle arrest and apoptosis mechanisms in response to DNA damage. Mutants of Casein Kinase 2 have impaired sperm development, which is particularly interesting since FAM134B protein is most dominant in testes tissues in humans and mice [19] [36] and this kinase is involved in cell cycle control, DNA repair, circadian rhythm, and the Wnt pathway.

5. DISCUSSION AND CONCLUSION

Perhaps the most interesting finding during the course of this study was the dramatic loss of thapsigargin and adriamycin resistance in Snu449 cells upon silencing of FAM134B. This result, as well as the other conclusions will be summarized and discussed in detail in this chapter.

5.1 Domains and Motifs found on the FAM134B Protein

Based on the domains and motifs on the protein products, FAM134B may be an ER-associated, reticulon-like, organelle shaping protein that may be subject to phosphorylation. FAM134B showed a perinuclear staining like that of calnexin, which may further implicate localization on the ER. Motif analyses indicated that the FAM134B protein has consensus sequence motifs that may be targeted for phosphorylation by important kinases such as ERK1 kinase, ATM kinase, Calmodulin dependent kinase 2, Casein kinase and 14-3-3 mode 1. These results may create a slightly clearer picture when combined with the SRB results that implicate a role for FAM134B in resistance to cytotoxic agents that inhibit calcium pumps on the ER membrane, and will be discussed in detail, along with further analyses that needs to be performed.

5.2 FAM134B and ER Stress

In mouse liver tissues, ER stress induction for 8 hours with tunicamycin does not cause an increase in FAM134B mRNA or protein levels. ER stress induction in 4 HCC cell lines with 3 different ER stress inducers for 3 different time points did not appear to cause a significant elevation in FAM134B mRNA and protein levels, except for 6 hours of 5mM DTT treatment on Snu449 cells, which also appeared to induce apoptosis.

5.3 FAM134B and Epithelial-to-Mesenchymal Transition

In HCC cell lines, the poorly-differentiated, more mesenchymal-like cell lines demonstrated higher FAM13B levels compared to the well-differentiated, more epithelial-like cell lines. EMT induction with TGF-β treatment resulted in a dramatic increase in the vimentin levels and mesenchymal-like morphology of PLC cells, accompanied by an increase in FAM134B protein levels.

Snu449 cells in which FAM134B was silenced through shRNA interference exhibited an altered morphology in cell culture, having a more elongated appearance compared to parental Snu449 cells and Snu449 cells transfected with Scrambled shRNA controls. However, the FAM13B silenced cells did not have a significant elevation in their vimentin levels. In fact, the FAM134B knockdown cells demonstrated less motility in a wound healing assay.

The loss of migratory capabilities upon knockdown of FAM134B may be the most interesting result related to EMT, since FAM134B levels are also observed to be elevated in the more mesenchymal-like HCC cell lines compared to the more epithelial-like ones. Previous research in our lab demonstrated that overexpression of FAM134B does not confer mesenchymal characteristics to Huh7 cells such as elevated vimentin expression [40].

Therefore, FAM134B may not be a cause but a result of EMT, and may be allowing cells that have gone through epithelial-to-mesenchymal transition to adapt to this new state, perhaps through shaping the ER membrane to a state that allows the mesenchymal state to persist, because when FAM134B is silenced, the cells lose their migratory capabilities.

5.4 FAM134B and Survival under Cytotoxic Stimuli

Knockdown of FAM134B in Snu449 cells resulted in a dramatic loss of resistance to thapsigargin and adriamycin treatment, which are both known to inhibit the functioning of the sarco-endoplasmic reticulum ATPases that constitute a channel on the ER membrane which is responsible for sequestering calcium from the cytosol and

regulating calcium homeostasis both in the ER and in the cytoplasm. With tunicamycin, the half maximal inhibitory concentration (IC_{50}) for Snu449 Scrambled4 cells was ~93nM, while only ~5nM was the half maximal inhibitory concentration for Snu449 shFAM134B 59-11 cells. With lower doses of adriamycin, the IC_{50} value for Snu449 Scrambled4 cells was ~747ng/ml, while it was only ~46ng/ml for Snu449 shFAM134B 59-11 cells. These results show a drastic 19 fold decrease in resistance to thapsigargin, and 16 fold reduction in resistance to adriamycin in FAM134B-silenced Snu449 cells.

The TGF-β cytotoxicity results were also very interesting, showing a 20 fold difference. With the TGF-β treatments, the IC_{50} value for Snu449 Scrambled4 cells was ~107ng/ml, while only ~5ng/ml TGF-β was enough for 50% inhibition in Snu449 shFAM134B 59-11 cells. Combined with the EMT-related observations, this result may implicate that while the control Snu449 cells are in a more mesenchymal-like state where TGF-β is not cytotoxic but is triggering other consequences in the cell, the FAM134B-silenced Snu449 cells are no longer able to accommodate a mesenchymal-like state and TGF-β treatment ends up being cytotoxic, probably causing cell cycle arrest and apoptosis, which may need to be further established.

FAM134B silencing also had some influence on cell survival under tunicamycin and ethanol treatment, inducing a 2 to 3 fold change in IC_{50} values. With tunicamycin, the IC_{50} value for Snu449 Scrambled4 cells was ~107ng/ml, and it was ~53ng/ml for Snu449 shFAM134B 59-11 cells. With ethanol, the IC_{50} value for Snu449 Scrambled4 cells was ~166mM, and it was ~72mM for Snu449 shFAM134B 59-11 cells. These may also implicate an ER-related role for FAM134B since tunicamycin is an ER stress inducer that works through inhibition of N-glycosylation, and ethanol challenges the cell to increase its smooth ER capacity for detoxification [27]. Therefore, when FAM134B is silenced, the cell may be rendered incapable of increasing its ER capacity to overcome these ER related challenges.

FAM134B silencing did not have a very significant influence on the resistance of Snu449 cells to other cytotoxic drugs and stimuli tested, such as H_2O_2, camptothecin, and 5-FU. Compared to the thapsigargin and adriamycin results, this may strengthen the hypothesis that FAM134B may specifically have a calcium related function.

Further experiments will need to be performed to fully confirm the effect of FAM134B knockdown in resistance to drugs such as Thapsigargin, and to better understand the function of this protein. Some of these experiments that need to be performed are described in the "Future Perspectives" section.

5.5 A Possible Relationship between the Src/PI3K and MEK1/ERK Pathways, the ER, FAM134B, and Calcium Homeostasis

It is important to state that this section is speculative, and not based on any experimental data obtained during the course of this thesis work. This section predicts the possibility of a role for FAM134B in cell survival under treatments with drugs such as thapsigargin that disturb calcium homeostasis, merely based on the knowledge available in the literature, and on the predictive online tool MotifScan. Further experimental research will need to be carried out in order to establish a function for the FAM134B protein, especially in the context of HCC.

The influence that FAM134B appears to have on survival under ER stress, especially when it is induced by disruption of calcium homeostasis, guided us towards inquiring more about mechanisms of survival under ER stress. A 2004 publication titled "Critical Role of Endogenous Akt/IAPs and MEK1/ERK Pathways in Counteracting Endoplasmic Reticulum Stress-induced Cell Death" investigated the mechanisms involved in survival under thapsigargin and tunicamycin induced ER stress. They demonstrated that inhibition of PI3K and the MEK1/ERK pathways sensitized MCF-7 and H1299 cells to thapsigargin- and tunicamycin-induced cell death, and that PI3K promoted survival both through Akt and through cross-talk with ERK. [25]

This is particularly interesting because Snu449 cells, which we observed to have a very high resistance to thapsigargin-induced apoptosis, were demonstrated to have elevated levels of endogenous Src activity, according to the 2005 article, "Biology of SNU Cell Lines" published by Seoul National University researchers that developed the SNU cell lines [55], and Src is a tyrosine kinase that is upstream of PI3K/Akt. Therefore, an elevated Src activity may imply an elevated PI3K activity, which may promote the resistance of Snu449 cells to thapsigargin, through Akt and ERK.

As presented earlier in the results section, the online MotifScan tool of the MIT predicted that ERK1 kinase may be phosphorylating FAM134B protein isoform 1. The predictions made by this tool has been successfully confirmed with experiments in several publications, such as the 2011 article published by Sharpe et al. which demonstrates that Akt phosphorylates a component of the coat protein II that mediates ER-to-Golgi trafficking [54].

The FAM134B protein appears to be localized on the cis compartment of the Golgi apparatus [57], which is the side that faces the ER, and also appears to have a function that is associated with the calcium pumps on the ER. Therefore, FAM134B may also be involved with the membrane-enclosed vesicles that are trafficked between the ER and the Golgi apparatus. Coat-protomer, or coatomer, proteins are the proteins that form the vesicles that are trafficked between the ER and the Golgi. COPI vesicles are responsible for transport from the Golgi back to the ER; this is usually performed to return misfolded proteins back to the ER because the Golgi apparatus has no chaperones and cannot accommodate proper protein folding. The transport from the ER to the Golgi apparatus, on the other hand, is carried out by the COPII vesicles. [54]

Interestingly, calcium gradients in the cytosol appear to influence the timing of the coating and uncoating of these vesicles that are transported between the ER and Golgi, as demonstrated by the article titled "A Role for Calcium in Stabilizing Transport Vesicle Coats" [29]. When cytosolic calcium is too high, the vesicles may not be able to uncoat to deliver their cargo.

The proteolytic enzyme called calpain 8 also functions in releasing the COP vesicles from the Golgi, and is interestingly regulated by cytosolic calcium as well. Excessive cytosolic calcium makes calpain excessively active, causing proteolysis of non-target proteins.

Taking these into consideration, further research has to be performed in order to determine the function of the FAM134B protein and to be able to place it in a pathway by identifying its possible upstream effectors.

6. FUTURE PERSPECTIVES

Before a conclusion can be reached on the function of the FAM134B protein, especially in the context of hepatocellular carcinoma, further research has to be conducted.

The effect of FAM134B silencing in resistance to drugs such as thapsigargin and adriamycin needs to be confirmed initially by using the other clones that have successfully silenced FAM134B protein levels; the Snu449 Scrambled 2 and Snu449 shFAM134B 59-12 clones may be another pair of clones that can be used, because the Snu449 shFAM134B 59-12 clones also had higly reduced levels of fAM134B, as demonstrated in Figure 4.14.

The impact of silencing FAM134B on resistance to cytotoxic drugs will also need to be further confirmed with siRNA transfection of Snu449 cells as well, because the process of constructing stable cell lines with shRNA transfection involves the selection of single cells and forming clones, and this individual cell may have alterations other than the silencing of FAM134B which may affect the findings, this is called “clonal effect”.

Another aspect that needs to be answered is whether FAM134B confers resistance to apoptosis by calcium pump inhibitors through actually preventing the inhibition of these pumps, or by accommodating the cell to these changes in calcium homeostasis. If FAM134B prevents the inhibition of calcium pumps, under thapsigargin and adriamycin treatment, the Snu449 cells should still have a high calcium concentration in the ER and lower levels of calcium in the cytosol, however, if the inhibition of the calcium pumps is not prevented, the cells will have low ER calcium levels and high cytosolic calcium levels. This can easily be established by using the calcium staining dye Alizarin Red.

The possible influences of Src, PI3K, and MEK/ERK on FAM134B protein levels and phosphorylation levels may be analyzed by initially using the inhibitors of these proteins, which are PP2/PP1 or Sarcatinib for Src, LY294002 for PI3K, and U0126

for MEK/ERK. Later, in order to investigate a direct interaction and phosphorylation of FAM134B protein by these kinases, co-immunoprecipitation and kinase assays would have to be performed.

Other HCC cell lines that may have endogenously hyperactive Src/PI3K and MEK1/ERK pathways may also be utilized to perform the experiments we have performed with Snu449 cells as well. For instance, Mahlavu cells have been shown to have hyper-phosphorylated Akt in previous studies, [58] therefore, Mahlavu cells may be a good candidate. Knockdowns in such other HCC cell lines and pathway analyses using inhibitors of possible upstream kinases of FAM134B may be ideal for being able to generalize our results to further HCC cell lines.

The results of these analyses may help determine the function of the FAM134B protein, place it in a pathway and understand how it may influence hepatocellular carcinoma.

7. REFERENCES

[1] J. Ferlay, H.-R. Shin, F. Bray, D. Forman, C. Mathers, and D. M. Parkin, "Estimates of worldwide burden of cancer in 2008: GLOBOCAN 2008.," *International journal of cancer Journal international du cancer*, vol. 127, no. 12, pp. 2893–2917, 2010.

[2] L. Faloppi, M. Scartozzi, E. Maccaroni, M. Di Pietro Paolo, R. Berardi, M. Del Prete, and S. Cascinu, "Evolving strategies for the treatment of hepatocellular carcinoma: from clinical-guided to molecularly-tailored therapeutic options.," *Cancer treatment reviews*, vol. 37, no. 3, pp. 169–77, May 2011.

[3] A. Jemal, F. Bray, M. M. Center, J. Ferlay, E. Ward, and D. Forman, "Global cancer statistics.," *CA a cancer journal for clinicians*, vol. 61, no. 2, pp. 69–90, 2011.

[4] S. F. Altekruse, K. a McGlynn, and M. E. Reichman, "Hepatocellular carcinoma incidence, mortality, and survival trends in the United States from 1975 to 2005.," *Journal of clinical oncology : official journal of the American Society of Clinical Oncology*, vol. 27, no. 9, pp. 1485–91, Mar. 2009.

[5] U. of W. S. of M. Dugdale, David C., MD and M. G. H. Chen, Yi-Bin, MD, "Hepatocellular carcinoma," 2011. [Online]. Available: http://cancercenternd.com/pdf/HepatocellularCarcinoma-CanceroftheLiver.pdf.

[6] G. C. Sotiropoulos, E. Tagkalos, I. Fouzas, S. Vernadakis, Z. Mathé, J. Treckmann, and A. Paul, "Liver Transplantation for Hepatocellular Carcinoma Using Extended Criteria Donor Grafts," *Transplantation proceedings*, vol. 44, no. 9. Elsevier Science Inc.,, pp. 2730–2733, 01-Nov-2012.

[7] R. Aravalli, "Development of MicroRNA Therapeutics for Hepatocellular Carcinoma," *Diagnostics*, vol. 3, no. 1, pp. 170–191, Mar. 2013.

[8] A. Soto-Gutierrez, H. Basma, N. Navarro-Alvarez, B. E. Uygun, M. L. Yarmush, N. Kobayashi, and I. J. Fox, "Differentiating Stem Cells into Liver," *Biotechnology and Genetic Engineering Reviews*, vol. 25, no. 1, pp. 149–164, Jan. 2008.

[9] M.-P. Bralet, V. Pichard, and N. Ferry, "Demonstration of direct lineage between hepatocytes and hepatocellular carcinoma in diethylnitrosamine-treated rats.," *Hepatology (Baltimore, Md.)*, vol. 36, no. 3, pp. 623–30, Sep. 2002.

[10] S. Badvie, “Hepatocellular carcinoma.,” *Postgraduate medical journal*, vol. 76, no. 891, pp. 4–11, Jan. 2000.

[11] S. Parikh and D. Hyman, “Hepatocellular cancer: a guide for the internist.,” *The American journal of medicine*, vol. 120, no. 3, pp. 194–202, Mar. 2007.

[12] P. A. Farazi and R. A. DePinho, “Hepatocellular carcinoma pathogenesis: from genes to environment,” *Nat Rev Cancer*, vol. 6, no. 9, pp. 674–687, Sep. 2006.

[13] S. Dooley and P. ten Dijke, “TGF-β in progression of liver disease.,” *Cell and tissue research*, vol. 347, no. 1, pp. 245–56, Jan. 2012.

[14] M. Ozturk, A. Arslan-Ergul, S. Bagislar, S. Senturk, and H. Yuzugullu, “Senescence and immortality in hepatocellular carcinoma.,” *Cancer letters*, vol. 286, no. 1, pp. 103–13, Dec. 2009.

[15] Mikulits, “Epithelial-mesenchymal transition in hepatocellular carcinoma,” *Future Oncol*, vol. 5, no. 8, pp. 1169–1179, 2009.

[16] K. Rombouts and F. Marra, “Molecular mechanisms of hepatic fibrosis in non-alcoholic steatohepatitis.,” *Digestive diseases (Basel, Switzerland)*, vol. 28, no. 1. pp. 229–35, Jan-2010.

[17] S. L. Friedman, “Evolving challenges in hepatic fibrosis.,” *Nature reviews. Gastroenterology & hepatology*, vol. 7, no. 8, pp. 425–36, Aug. 2010.

[18] J. M. Gartner, Leslie P. Hiatt, James L. Strum, *Cell biology and histology.*, 5th ed. Lippincott Williams & Wilkins., 2007, p. 83.

[19] G. C. Blobe, W. P. Schiemann, and H. F. Lodish, “Role of Transforming Growth Factor β in Human Disease,” *New England Journal of Medicine*, vol. 342, no. 18, pp. 1350–1358, May 2000.

[20] M. Zeisberg, C. Yang, M. Martino, M. B. Duncan, F. Rieder, H. Tanjore, and R. Kalluri, “Fibroblasts Derive from Hepatocytes in Liver Fibrosis via Epithelial to Mesenchymal Transition,” *Journal of Biological Chemistry* , vol. 282 , no. 32 , pp. 23337–23347, Aug. 2007.

[21] T. Nitta, J.-S. Kim, D. Mohuczy, and K. E. Behrns, “Murine cirrhosis induces hepatocyte epithelial mesenchymal transition and alterations in survival signaling pathways,” *Hepatology*, vol. 48, no. 3, pp. 909–919, Sep. 2008.

[22] S. Dooley, J. Hamzavi, L. Ciuclan, P. Godoy, I. Ilkavets, S. Ehnert, E. Ueberham, R. Gebhardt, S. Kanzler, A. Geier, K. Breitkopf, H. Weng, and P. R. Mertens, “Hepatocyte-specific Smad7 expression attenuates TGF-beta-mediated fibrogenesis and protects against liver damage.,” *Gastroenterology*, vol. 135, no. 2, pp. 642–659, Aug. 2008.

[23] A. Kaimori, J. Potter, J.-Y. Kaimori, C. Wang, E. Mezey, and A. Koteish, "Transforming growth factor-beta1 induces an epithelial-to-mesenchymal transition state in mouse hepatocytes in vitro.," *The Journal of biological chemistry*, vol. 282, no. 30, pp. 22089–101, Jul. 2007.

[24] P. Godoy, J. G. Hengstler, I. Ilkavets, C. Meyer, A. Bachmann, A. Müller, G. Tuschl, S. O. Mueller, and S. Dooley, "Extracellular matrix modulates sensitivity of hepatocytes to fibroblastoid dedifferentiation and transforming growth factor β–induced apoptosis," *Hepatology*, vol. 49, no. 6, pp. 2031–2043, Jun. 2009.

[25] P. Hu, Z. Han, A. D. Couvillon, and J. H. Exton, "Critical Role of Endogenous Akt / IAPs and MEK1 / ERK Pathways in Counteracting Endoplasmic Reticulum Stress-induced Cell Death *," vol. 279, no. 47, pp. 49420–49429, 2004.

[26] S. Fu, L. Yang, P. Li, O. Hofmann, L. Dicker, W. Hide, X. Lin, S. M. Watkins, A. R. Ivanov, and G. S. Hotamisligil, "Aberrant lipid metabolism disrupts calcium homeostasis causing liver endoplasmic reticulum stress in obesity.," *Nature*, vol. 473, no. 7348, pp. 528–31, May 2011.

[27] P. Alberts, Johnson, Lewis, Raff, Roberts, Walter, *Molecular Biology of the Cell*, 4th ed. New York: Garland Science, 2002.

[28] G. S. Hotamisligil, "Endoplasmic reticulum stress and the inflammatory basis of metabolic disease.," *Cell*, vol. 140, no. 6, pp. 900–17, Mar. 2010.

[29] J. P. Ahluwalia, J. D. Topp, M. Zimmerman, J. B. Chem, K. Weirather, and M. Stamnes, "A Role for Calcium in Stabilizing Transport Vesicle Coats A Role for Calcium in Stabilizing Transport Vesicle Coats *," 2001.

[30] H. Malhi and R. J. Kaufman, "Endoplasmic reticulum stress in liver disease.," *Journal of hepatology*, vol. 54, no. 4, pp. 795–809, Apr. 2011.

[31] A. Mandic, J. Hansson, S. Linder, and M. C. Shoshan, "Cisplatin induces endoplasmic reticulum stress and nucleus-independent apoptotic signaling.," *The Journal of biological chemistry*, vol. 278, no. 11, pp. 9100–6, Mar. 2003.

[32] S. Hummasti and G. S. Hotamisligil, "Endoplasmic reticulum stress and inflammation in obesity and diabetes.," *Circulation research*, vol. 107, no. 5, pp. 579–91, Sep. 2010.

[33] L. Ulianich, C. Garbi, A. S. Treglia, D. Punzi, C. Miele, G. A. Raciti, F. Beguinot, E. Consiglio, and B. Di Jeso, "ER stress is associated with dedifferentiation and an epithelial-to-mesenchymal transition-like phenotype in PC Cl3 thyroid cells.," *Journal of cell science*, vol. 121, no. Pt 4, pp. 477–86, Mar. 2008.

[34] Q. Zhong, B. Zhou, D. K. Ann, P. Minoo, Y. Liu, A. Banfalvi, M. S. Krishnaveni, M. Dubourd, L. Demaio, B. C. Willis, K.-J. Kim, R. M. duBois, E. D. Crandall, M. F. Beers, and Z. Borok, "Role of endoplasmic reticulum stress in epithelial-mesenchymal transition of alveolar epithelial cells: effects of misfolded surfactant protein.," *American journal of respiratory cell and molecular biology*, vol. 45, no. 3, pp. 498–509, Sep. 2011.

[35] S. H. Park and C. Blackstone, "Further assembly required: construction and dynamics of the endoplasmic reticulum network.," *EMBO reports*, vol. 11, no. 7, pp. 515–21, Jul. 2010.

[36] G. K. Voeltz, W. A. Prinz, Y. Shibata, J. M. Rist, and T. A. Rapoport, "A Class of Membrane Proteins Shaping the Tubular Endoplasmic Reticulum," *Cell*, vol. 124, no. 3, pp. 573–586, Feb. 2006.

[37] I. Kurth, T. Pamminger, J. C. Hennings, D. Soehendra, K. Antje, A. Rotthier, J. Baets, J. Senderek, H. Topaloglu, A. Sandra, G. Nürnberg, P. Nürnberg, P. De Jonghe, A. Gal, C. Kaether, V. Timmerman, and C. A. Hübner, "Mutations in FAM134B , encoding a novel Golgi protein , cause severe sensory and autonomic neuropathy."

[38] W. K. Tang, C. H. Chui, S. Fatima, S. H. L. Kok, K. C. Pak, T. M. Ou, K. S. Hui, M. M. Wong, J. Wong, S. Law, S. W. Tsao, K. Y. Lam, P. S. L. Beh, G. Srivastava, A. S. C. Chan, K. P. Ho, and J. C. O. Tang, "Oncogenic properties of a novel gene JK-1 located in chromosome 5p and its overexpression in human esophageal squamous cell carcinoma.," *International Journal of Molecular Medicine*, vol. 19, no. 6, pp. 915–923, 2007.

[39] L. Scheubert, R. Schmidt, D. Repsilber, M. Lustrek, and G. Fuellen, "Learning biomarkers of pluripotent stem cells in mouse.," *DNA research : an international journal for rapid publication of reports on genes and genomes*, vol. 18, no. 4, pp. 233–51, Aug. 2011.

[40] M. Yılmaz, "CHARACTERIZATION OF FAM134B IN THE CONTEXT OF HEPATOCELLULAR CARCINOMA AND ENDOPLASMIC RETICULUM STRESS," Bilkent University, 2011.

[41] N. Tasdemir, "IDENTIFICATION AND CHARACTERIZATION OF TWO ENDOPLASMIC RETICULUM PROTEIN ISOFORMS ENCODED BY SENESCENCE - ASSOCIATED FAM134B GENE," Bilkent University, 2008.

[42] H. Yuzugullu, K. Benhaj, N. Ozturk, S. Senturk, E. Celik, A. Toylu, N. Tasdemir, M. Yilmaz, E. Erdal, K. C. Akcali, N. Atabey, and M. Ozturk, "Canonical Wnt signaling is antagonized by noncanonical Wnt5a in hepatocellular carcinoma cells," vol. 20, pp. 1–20, 2009.

[43] M. Wictome, I. Henderson, A. G. Lee, and J. M. East, “Mechanism of inhibition of the calcium pump of sarcoplasmic reticulum by thapsigargin,” vol. 283, pp. 525–529, 1992.

[44] D. Xiao and J. He, “Epithelial mesenchymal transition and lung cancer.,” *Journal of thoracic disease*, vol. 2, no. 3, pp. 154–9, Sep. 2010.

[45] V. Vichai and K. Kirtikara, “Sulforhodamine B colorimetric assay for cytotoxicity screening,” *Nat. Protocols*, vol. 1, no. 3, pp. 1112–1116, Aug. 2006.

[46] K. Ondrias, L. Borgatta, D. H. Kim, and B. E. Ehrlich, “Biphasic effects of doxorubicin on the calcium release channel from sarcoplasmic reticulum of cardiac muscle,” *Circulation Research*, vol. 67, no. 5, pp. 1167–1174, Nov. 1990.

[47] S. Senturk, M. Mumcuoglu, O. Gursoy-Yuzugullu, B. Cingoz, K. C. Akcali, and M. Ozturk, “Transforming growth factor-beta induces senescence in hepatocellular carcinoma cells and inhibits tumor growth.,” *Hepatology (Baltimore, Md.)*, vol. 52, no. 3, pp. 966–74, Sep. 2010.

[48] K. D. Rodland, L. L. Muldoon, and B. E. Magun, “Cellular Mechanisms of TGF-[beta] Action,” *J Investig Dermatol*, vol. 94, no. s6, p. 33s–40s, Jun. 1990.

[49] Z. S. Lodish H, Berk A, *Molecular Cell Biology*, 4th ed. New York: , 2000.

[50] D. B. Longley, D. P. Harkin, and P. G. Johnston, “5-Fluorouracil: mechanisms of action and clinical strategies,” *Nat Rev Cancer*, vol. 3, no. 5, pp. 330–338, May 2003.

[51] L. F. LIU, S. D. DESAI, T.-K. LI, Y. MAO, M. E. I. SUN, and S.-P. SIM, “Mechanism of Action of Camptothecin,” *Annals of the New York Academy of Sciences*, vol. 922, no. 1, pp. 1–10, Dec. 2000.

[52] G. Barrera, “Oxidative stress and lipid peroxidation products in cancer progression and therapy.,” *ISRN oncology*, vol. 2012, p. 137289, Jan. 2012.

[53] J. C. Obenauer, “Scansite 2.0: proteome-wide prediction of cell signaling interactions using short sequence motifs,” *Nucleic Acids Research*, vol. 31, no. 13, pp. 3635–3641, Jul. 2003.

[54] L. J. Sharpe, W. Luu, and A. J. Brown, “Akt Phosphorylates Sec24 : New Clues into the Regulation of ER-to-Golgi Trafficking,” vol. 1, no. 3, pp. 19–27, 2011.

[55] J. Ku, J. Park, and D. Ph, “Biology of SN U C ell L ines,” vol. 37, no. 1, pp. 1–19, 2005.

[56] H. Liu, J. Xu, and L. Zhou, “Hepatitis B Virus Large Surface Antigen Promotes Liver Carcinogenesis by Activating the Src / PI3K / Akt Pathway,” pp. 7547–7557, 2011.

[57] I. Kurth, T. Pamminger, J. C. Hennings, D. Soehendra, K. Antje, A. Rotthier, J. Baets, J. Senderek, H. Topaloglu, A. Sandra, G. Nürnberg, P. Nürnberg, P. De Jonghe, A. Gal, C. Kaether, V. Timmerman, and C. A. Hübner, “Mutations in FAM134B , encoding a novel Golgi protein , cause severe sensory and autonomic neuropathy.”

[58] F. Buontempo, T. Ersahin, S. Missiroli, S. Senturk, and D. Etro, “Inhibition of Akt signaling in hepatoma cells induces apoptotic cell death independent of Akt activation status,” pp. 1303–1313, 2011.

[59] S. L. Friedman, “Evolving challenges in hepatic fibrosis.,” *Nature reviews. Gastroenterology & hepatology*, vol. 7, no. 8, pp. 425–36, Aug. 2010.

Licenses to copyrighted material

Licensee: Derya Soner
License Date: Jul 28, 2013
License Number: 3197561404733
Publication: Nature Reviews Cancer
Title: Hepatocellular carcinoma pathogenesis: from genes to environment
Type Of Use: reuse in a thesis/dissertation
Total: 0.00 USD

Licensee: Derya Soner
License Date: Jul 9, 2013
License Number: 3184781129039
Publication: Nature Reviews Gastroenterology and Hepatology
Title: Evolving challenges in hepatic fibrosis
Type Of Use: reuse in a thesis/dissertation
Total: 0.00 USD

Licensee: Derya Soner
License Date: Jul 29, 2013
License Number: 3198420498357
Publication: Circulation Research
Title: Endoplasmic Reticulum Stress and Inflammation in Obesity and Diabetes
Type Of Use: Dissertation/Thesis
Total: 0.00 USD